

Ice clouds: optical phenomena, optical properties and remote sensing

Bastiaan van Diedenhoven, GISS lunch seminar 2014

**Clouds associated
with Superstorm
Sandy's outflow**

Huntsville, AL, Oct. 30, 2012
(Earth Science Picture of the
Day, Nov. 12, 2012)



Three subjects

- Optical phenomena
 - van Diedenhoven: *The prevalence of the 22° halo in cirrus clouds*, JQSRT, in press
- Optical properties
 - Van Diedenhoven, B., A.S. Ackerman, B. Cairns, and A.M. Fridlind: *A flexible parameterization for shortwave optical properties of ice crystals*, J. Atmos. Sci., in press
- Remote sensing
 - Van Diedenhoven, B., B. Cairns, I.V. Geogdzhayev, A.M. Fridlind, A.S. Ackerman, P. Yang, and B.A. Baum: *Remote sensing of ice crystal asymmetry parameter using multi-directional polarization measurements — Part 1: Methodology and evaluation with simulated measurements*, Atmos. Meas. Tech., 2012
 - Van Diedenhoven, B., B. Cairns, A.M. Fridlind, A.S. Ackerman, and T.J. Garrett: *Remote sensing of ice crystal asymmetry parameter using multi-directional polarization measurements — Part 2: Application to the Research Scanning Polarimeter*. Atmos. Chem. Phys., 2013



Clouds are made of.....



A: Cotton balls



B: Ice cream



C: Water

Ice clouds: optical phenomena, optical properties and remote sensing

Bastiaan van Diedenhoven, GISS lunch seminar 2014

**Clouds associated
with Superstorm
Sandy's outflow**

Huntsville, AL, Oct. 30, 2012
(Earth Science Picture of the
Day, Nov. 12, 2012)



22-degree halo

Sassen et al., 2003:

- 10 year statistics in Salt Lake City
- 37% of ice clouds showed 22° halo
- 6% bright and prolonged



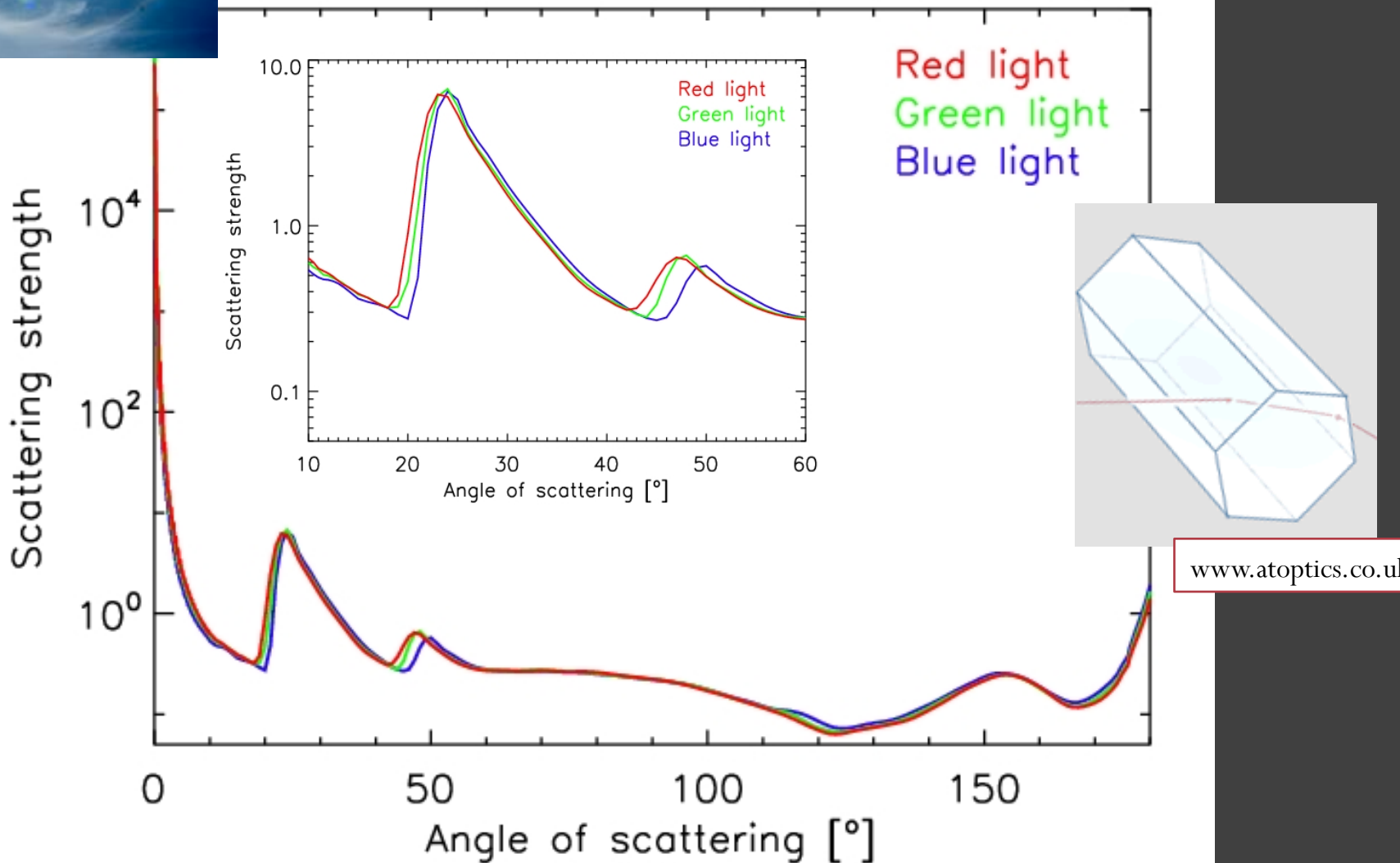
Around
moon



ER-2 aircraft during PODEX
campaign, NASA Dryden



22-degrees halo produced by randomly oriented smooth hexagonal ice crystals

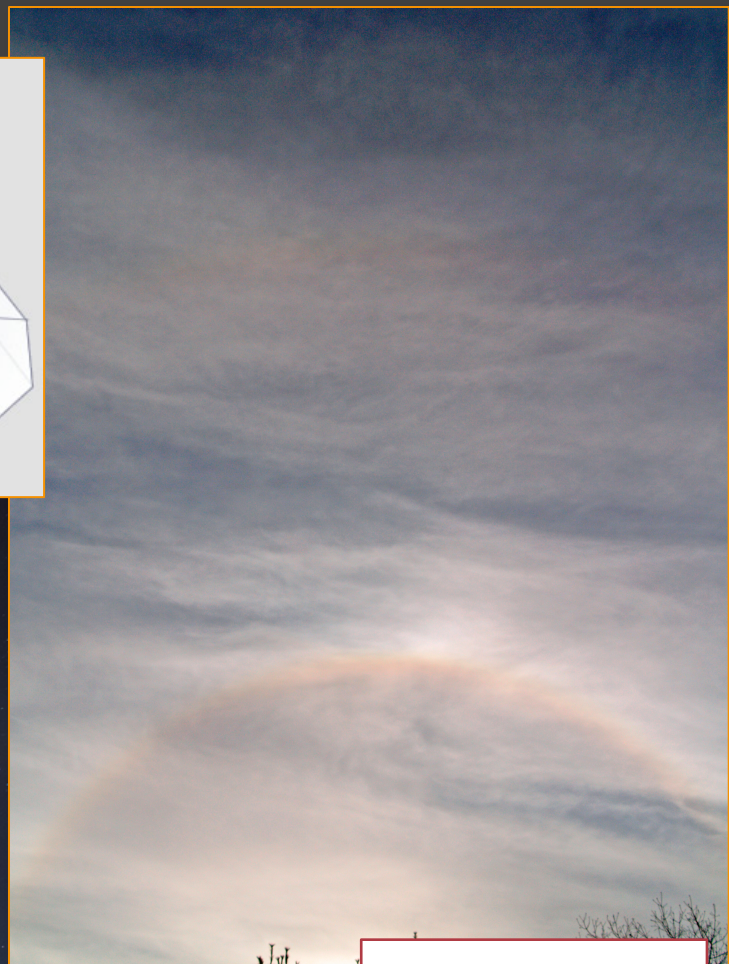
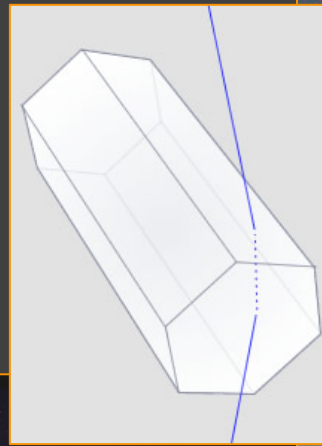


46 degree halo

Sassen et al., 2003:

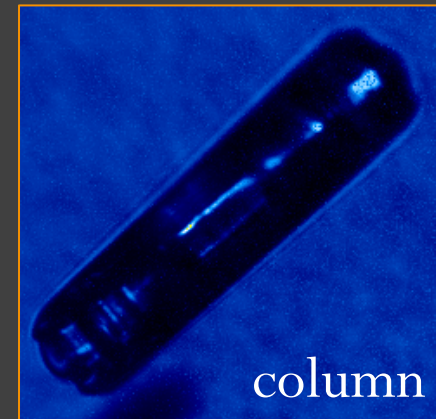
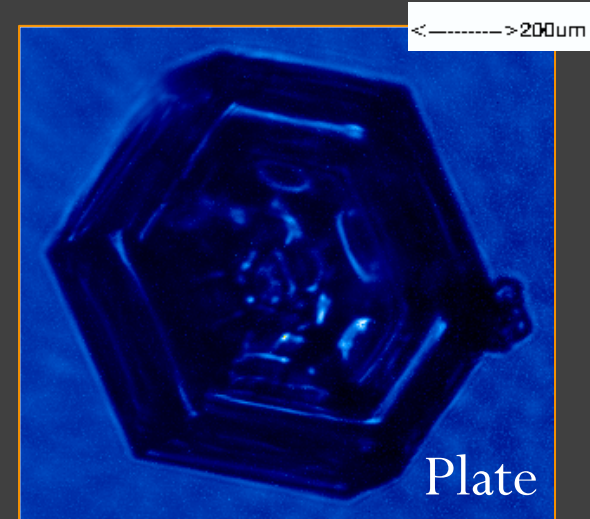
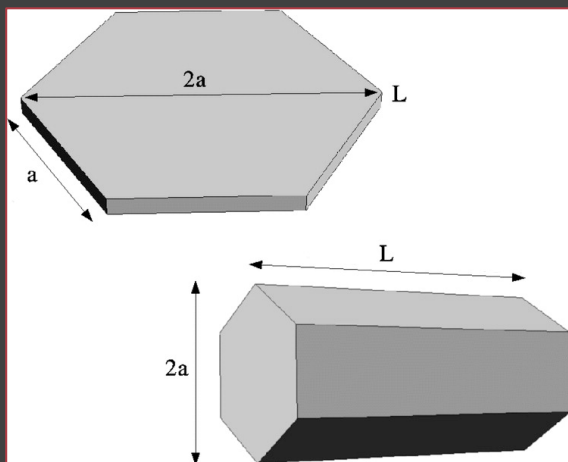
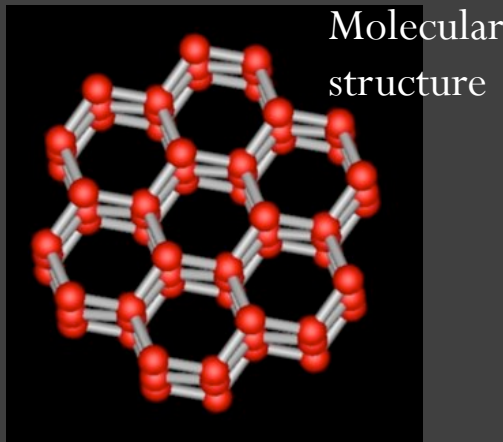
- Occurred in 0.4% of 10 year statistics
in Salt Lake City

Moon halos,
Finland



Earth Science
Picture of the
Day (May 29,
2012)

Hexagonal columns and plates are fundamental ice crystal shapes



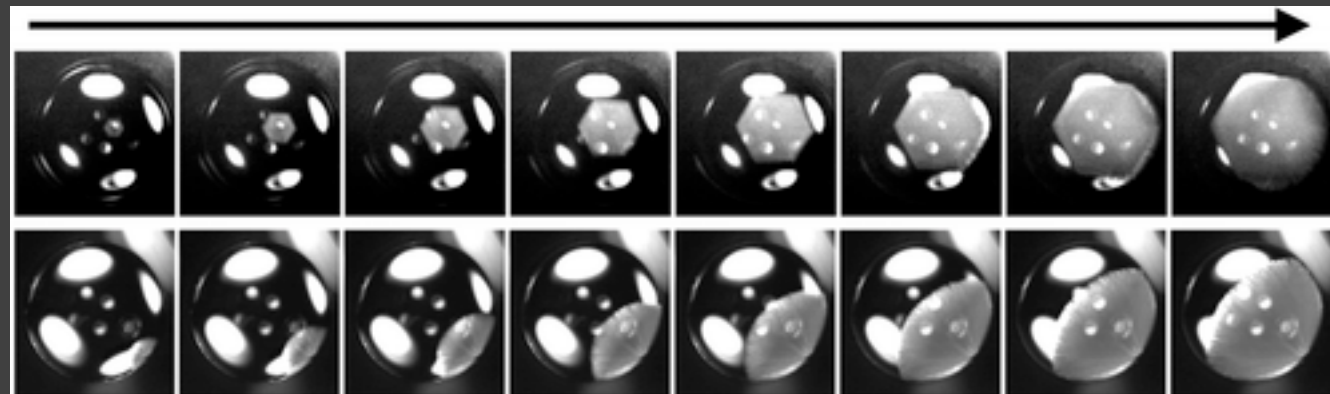
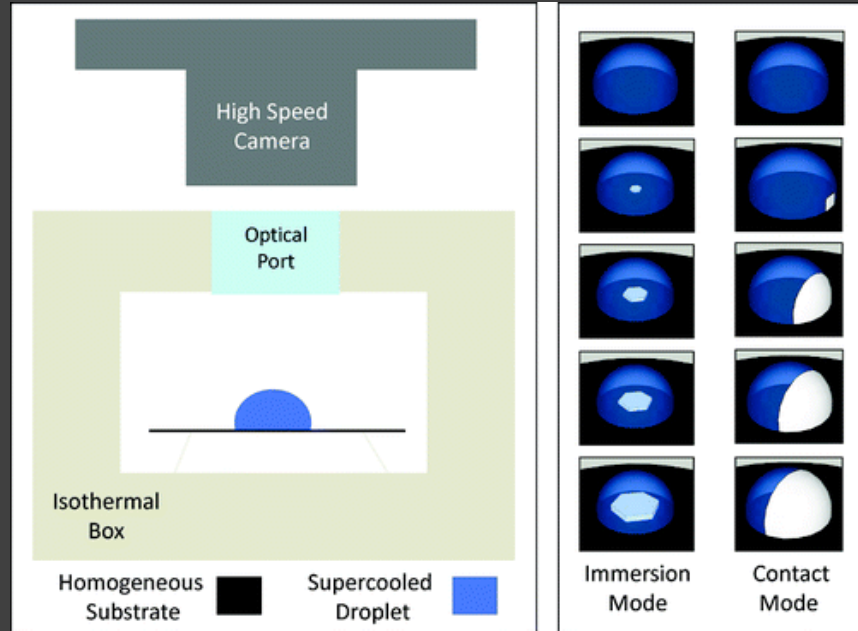
Freezing drops

Colin Gurganus , Alexander B. Kostinski ,
and Raymond A. Shaw

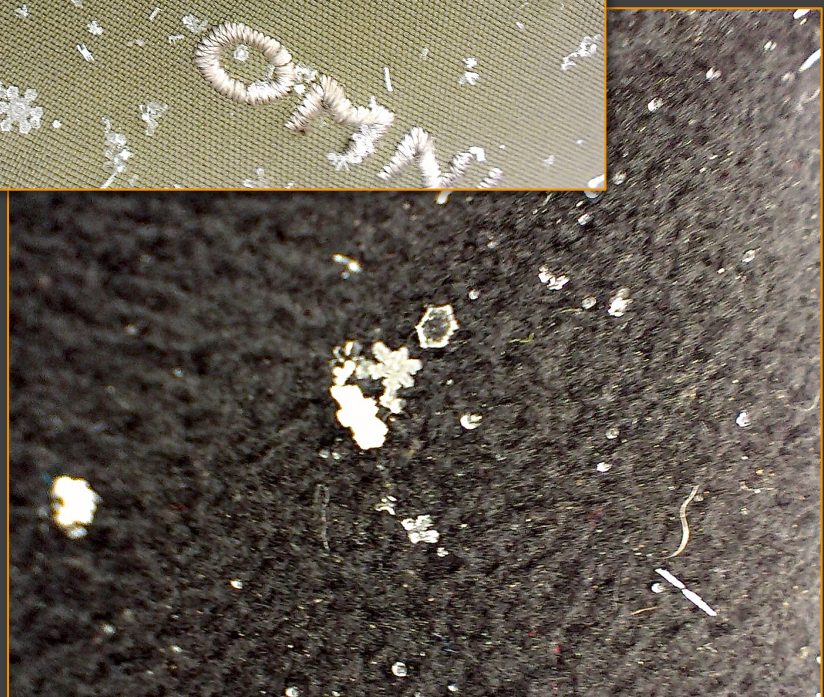
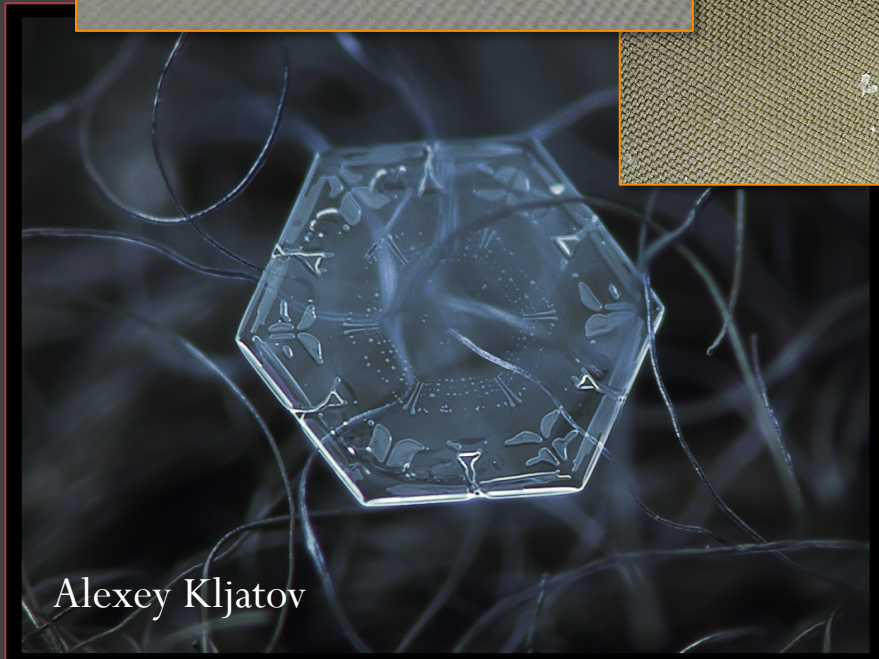
“Fast Imaging of Freezing Drops: No
Preference for Nucleation at the Contact
Line”

J. Phys. Chem. Lett. , 2011, 2 (12), pp 1449–1454

DOI: 10.1021/jz2004528

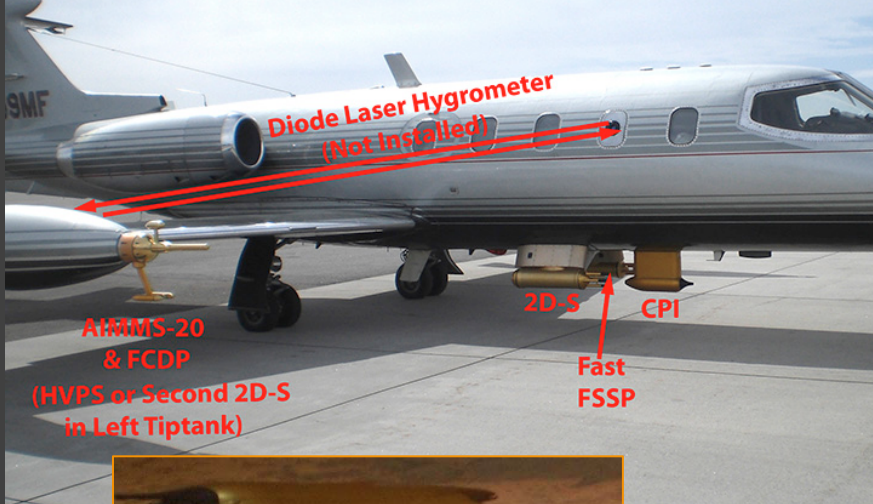


Movie available at <http://pubs.acs.org/doi/suppl/10.1021/jz2004528>



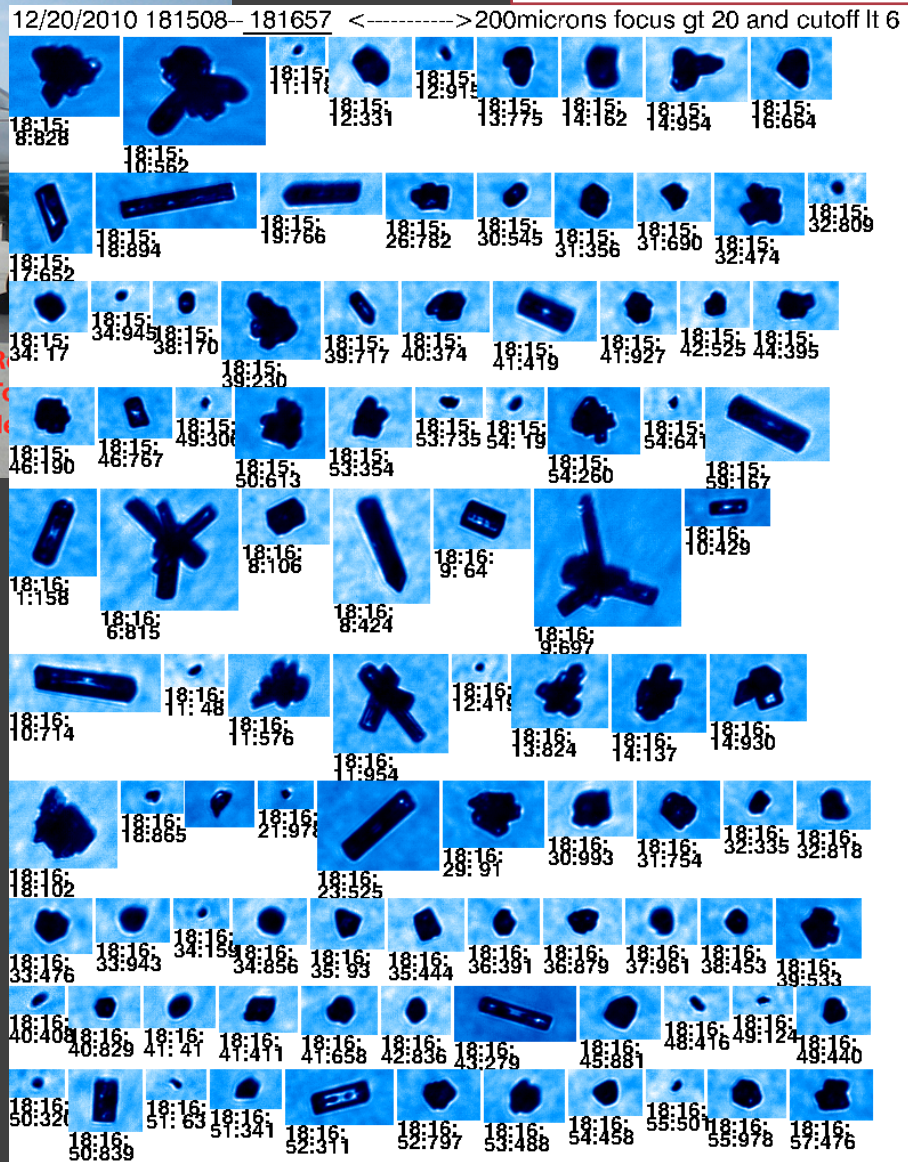
Cell phone pictures
taken on 3 Jan.
2014

SPEC Learjet



Cloud Particle Imager (CPI)

Sparticus campaign

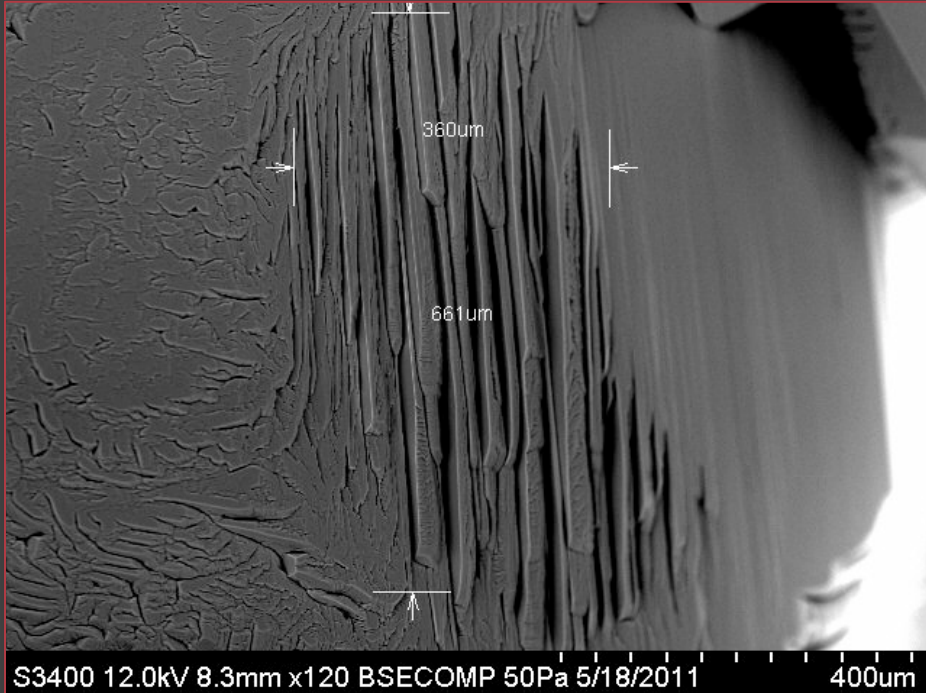


Cloud Particle Imager (CPI)

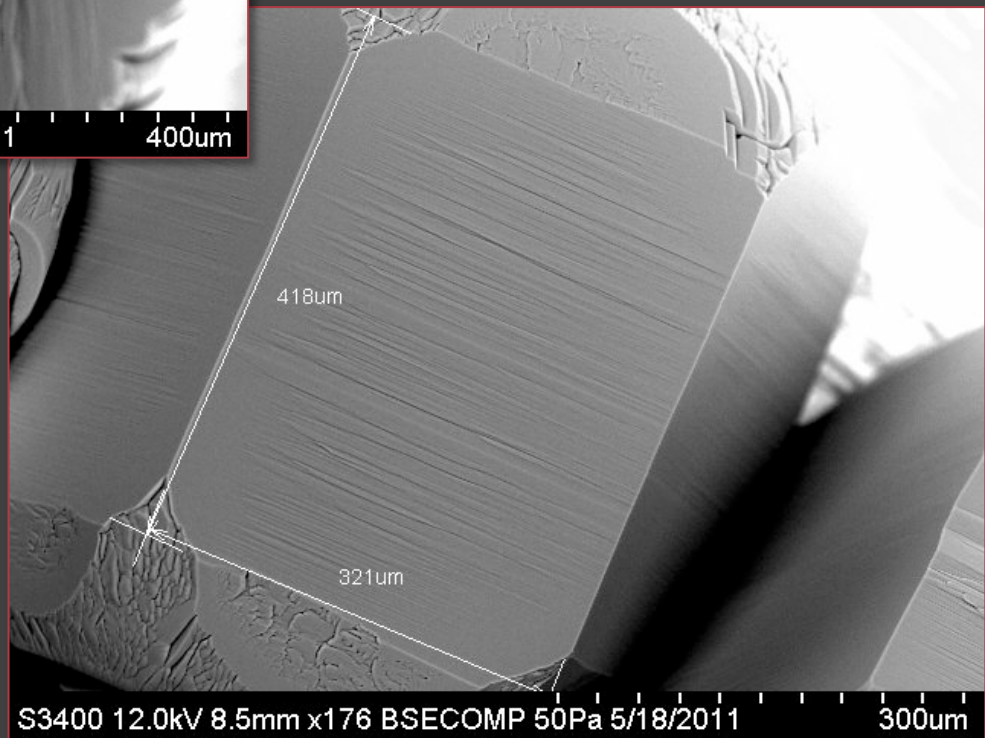


Sparticus campaign

Surface roughness

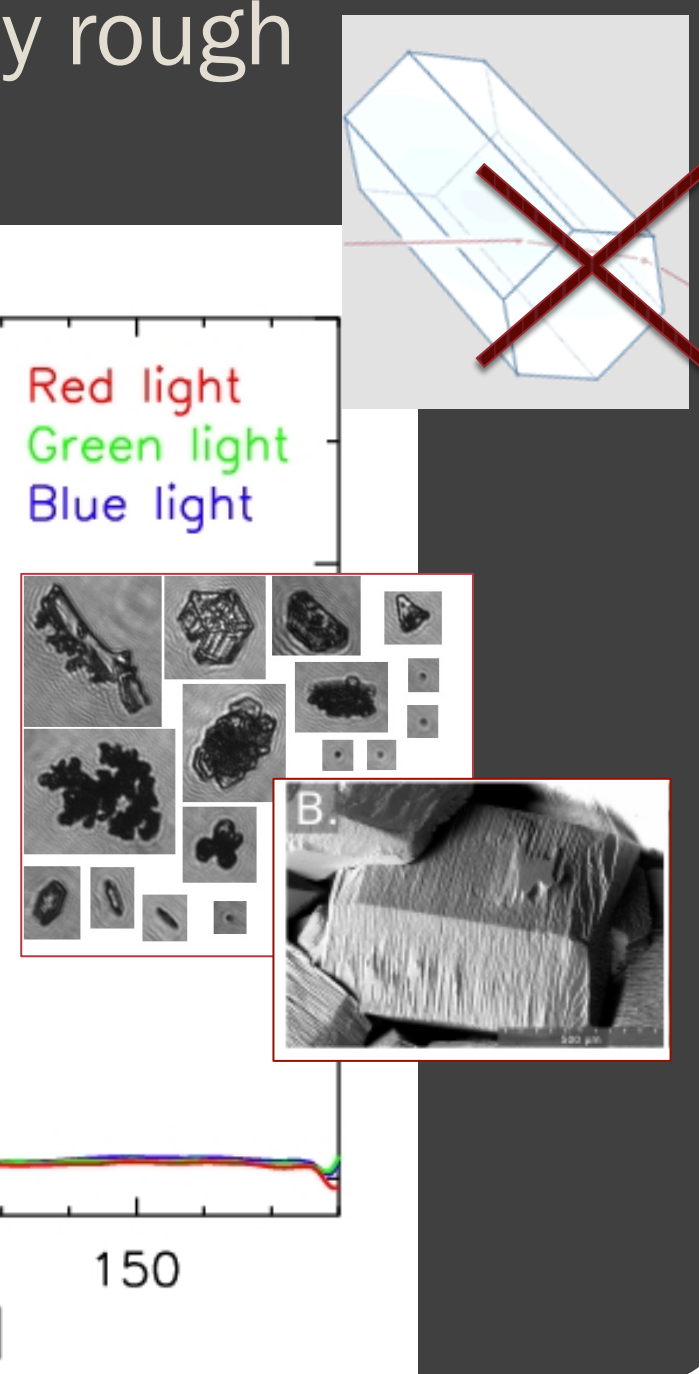
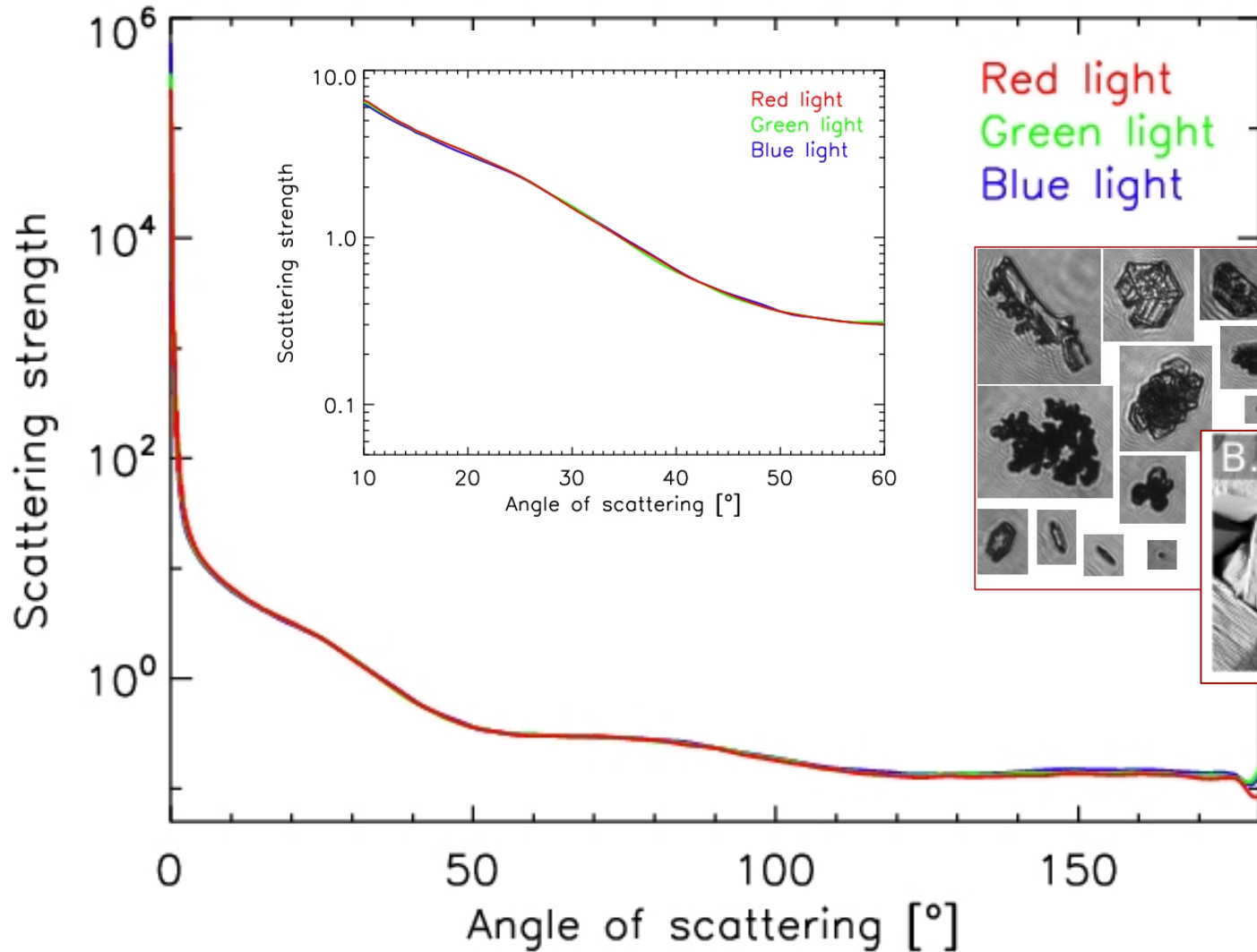


Scanning electron
microscope images from
Steven Neshyba,
University of Puget
Sound

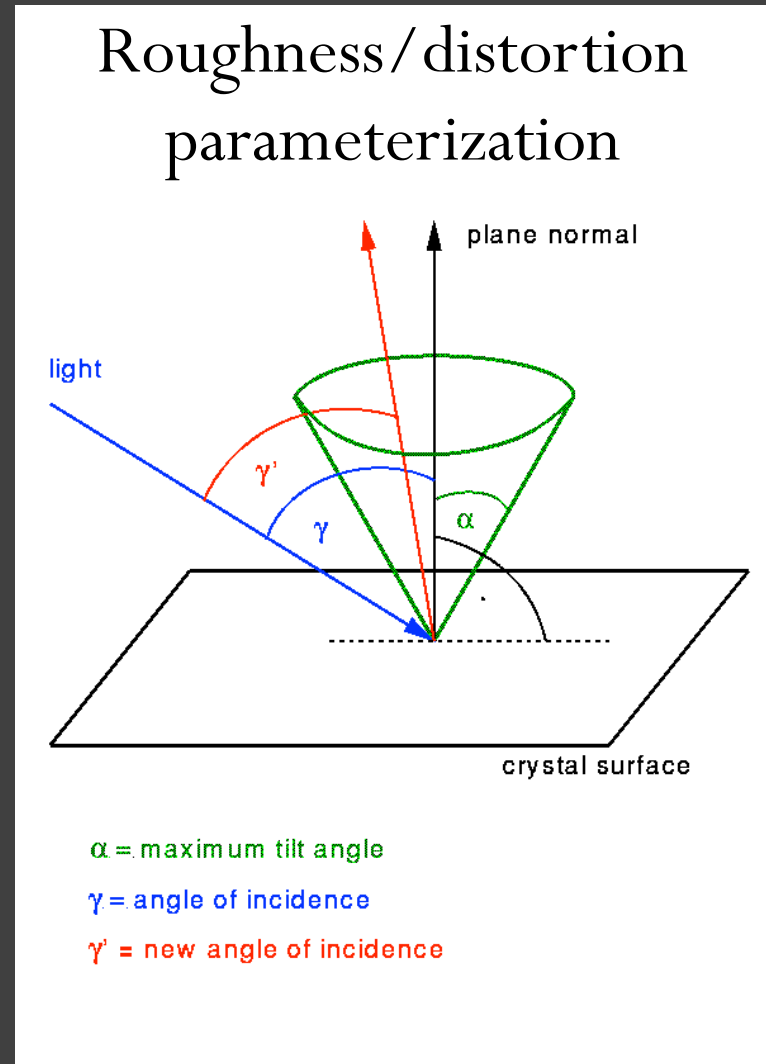
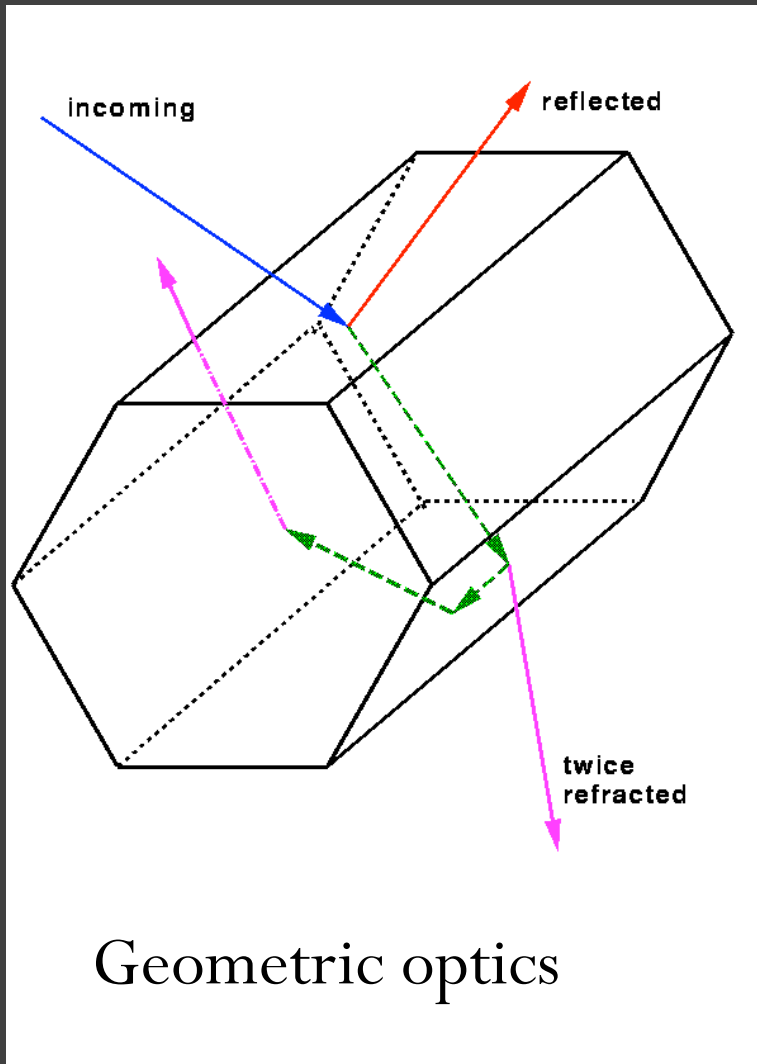




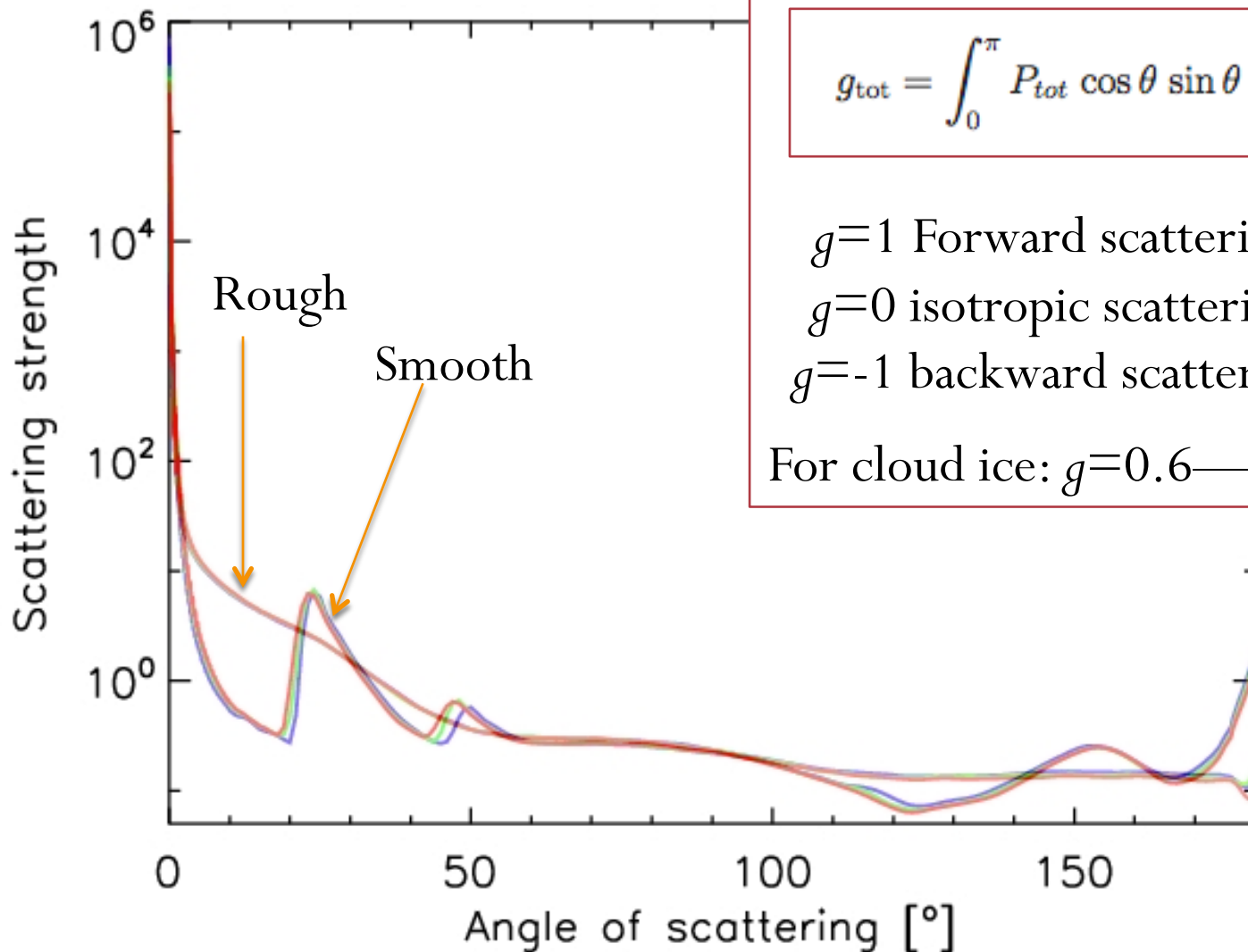
No halos produced by rough ice crystals



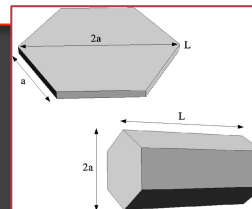
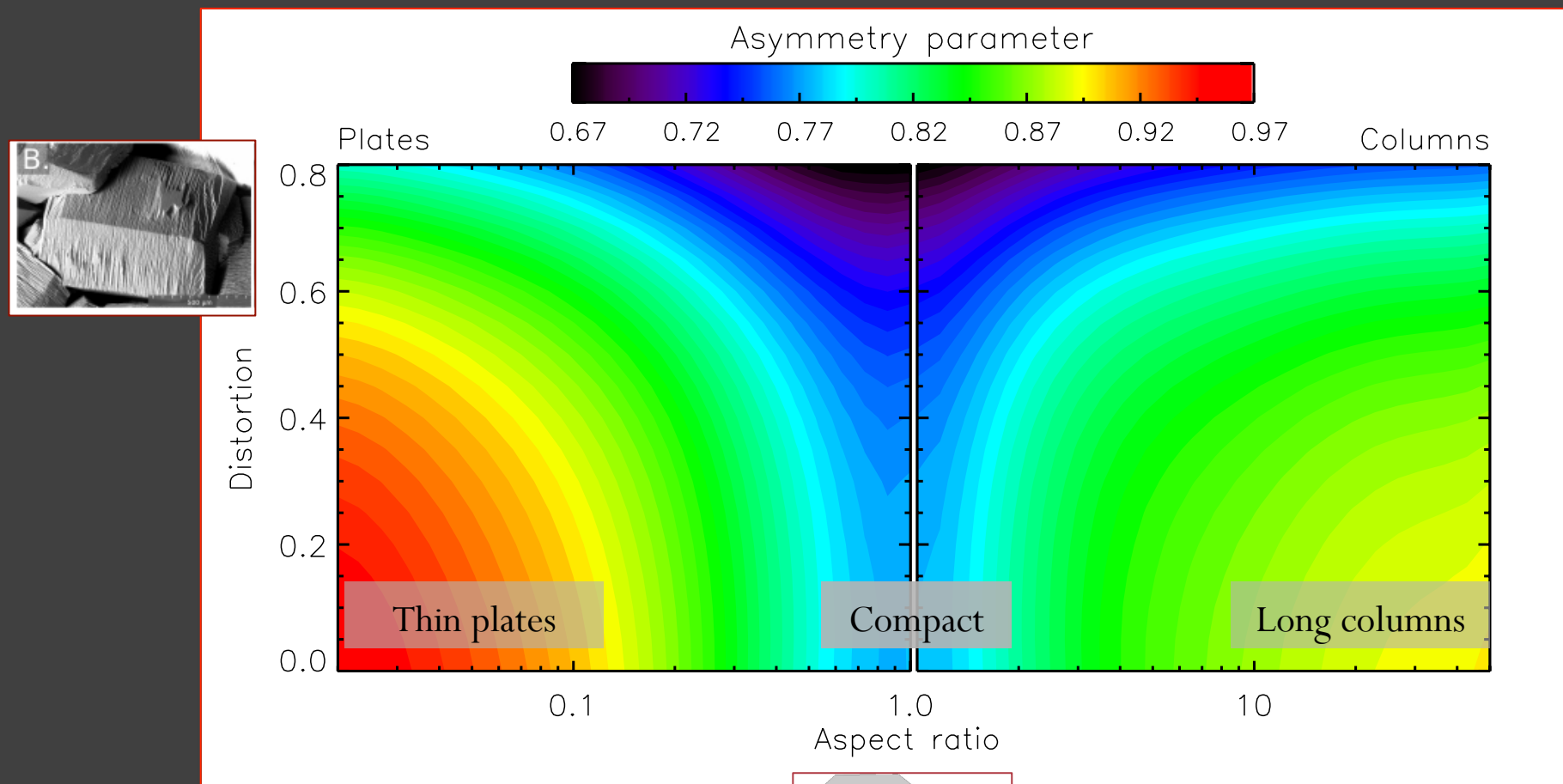
Ray tracing and simulating roughness/distortion (e.g., Macke et al 1996)



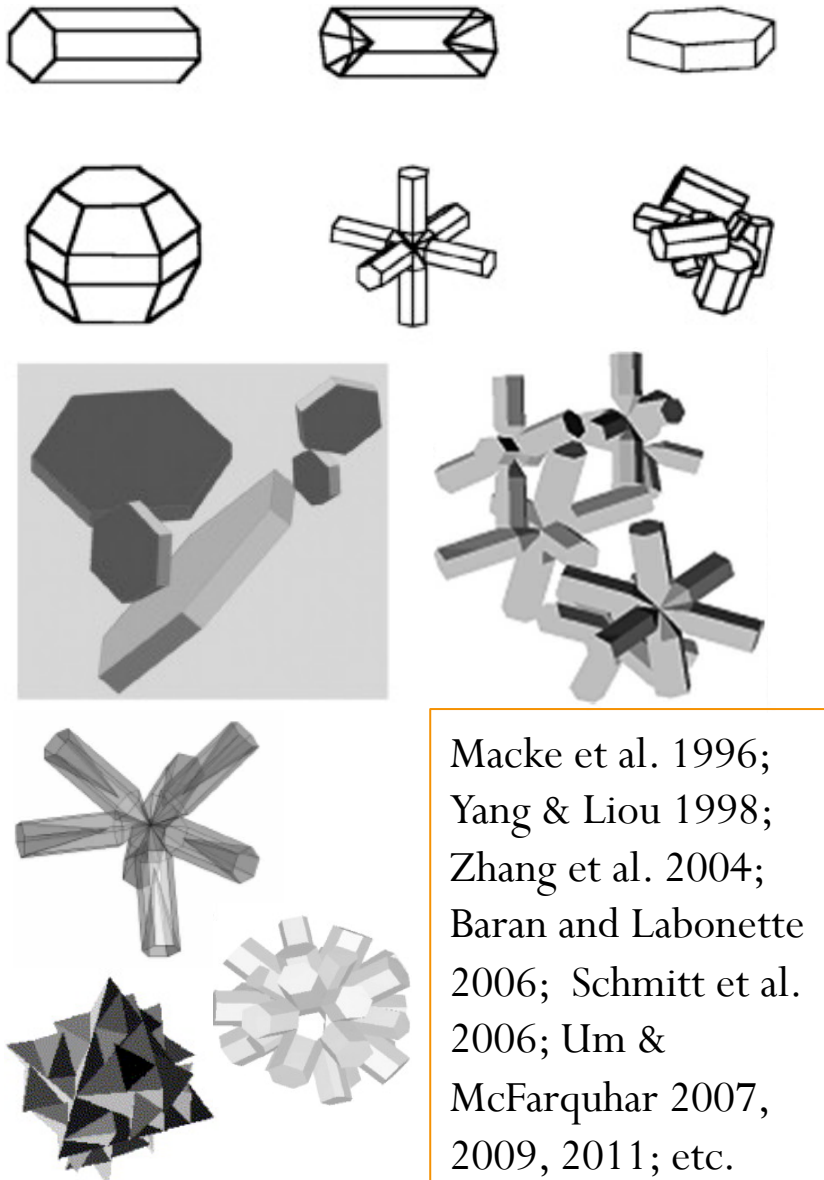
Smooth versus rough hexagonal ice crystals



Ice crystal asymmetry parameter dependence on aspect ratio and distortion



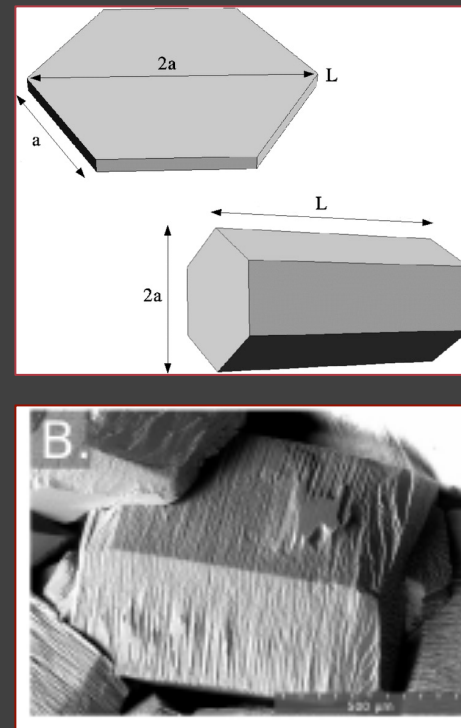
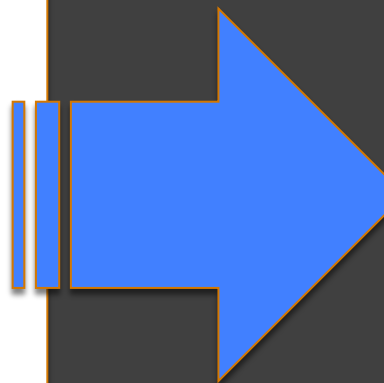
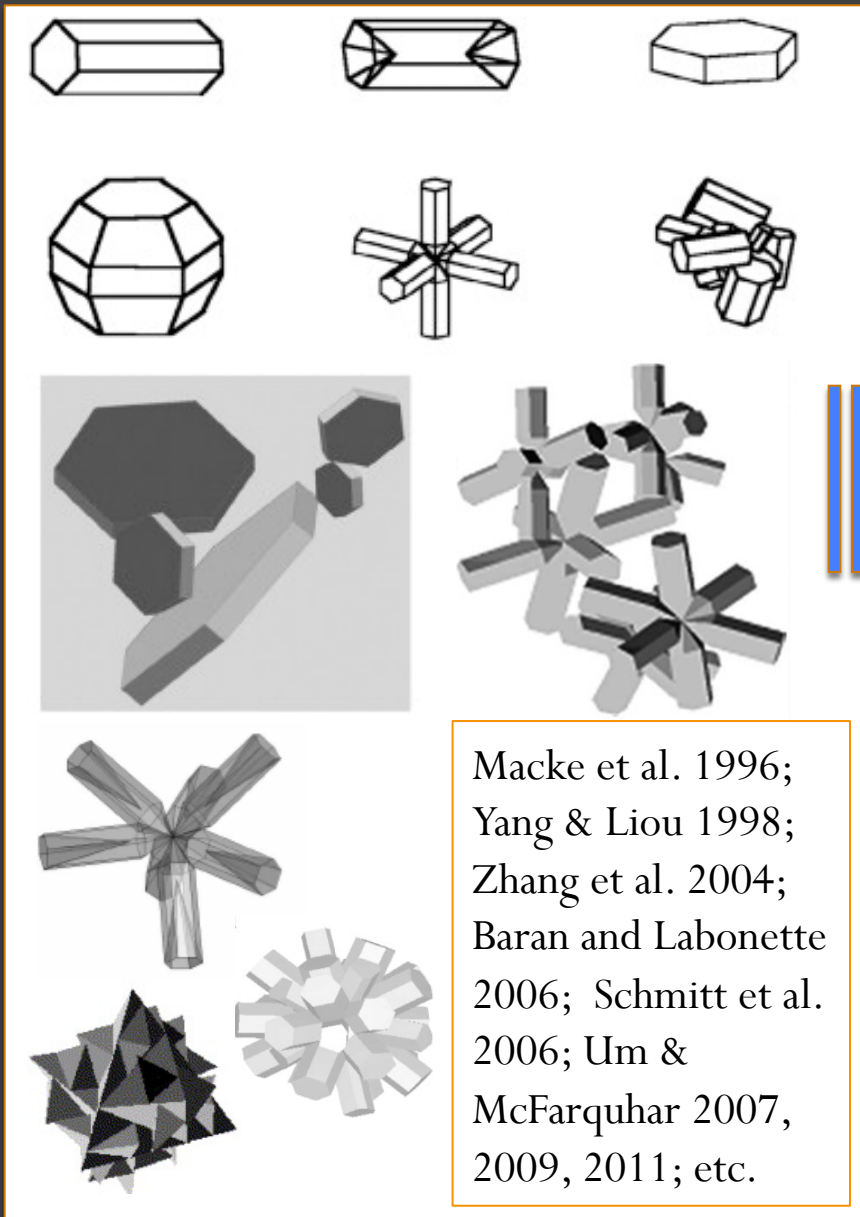
Simulating optical properties



Macke et al. 1996;
Yang & Liou 1998;
Zhang et al. 2004;
Baran and Labonette
2006; Schmitt et al.
2006; Um &
McFarquhar 2007,
2009, 2011; etc.



Breaking down complex ice into simple radiative proxies

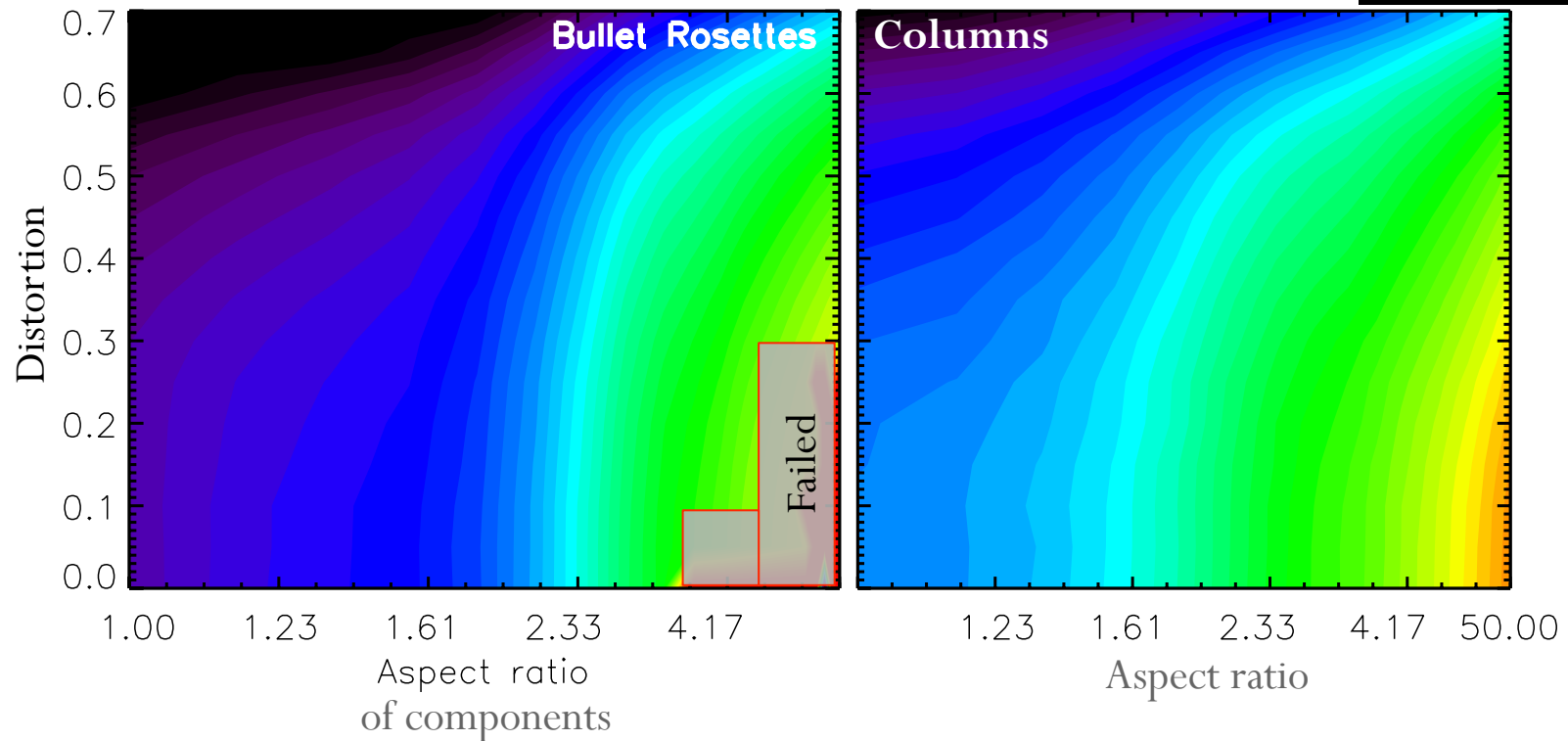
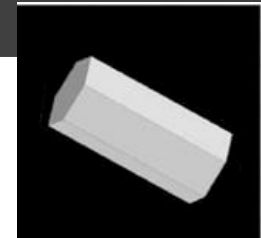
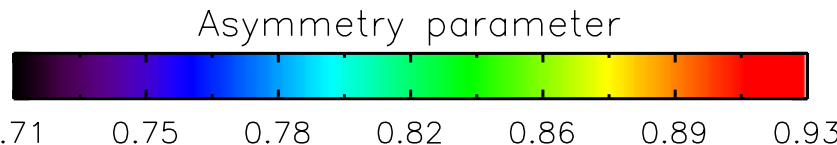
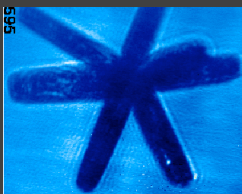


Scattering properties mainly depend on

- Aspect ratios of hexagonal components
- Crystal distortion levels

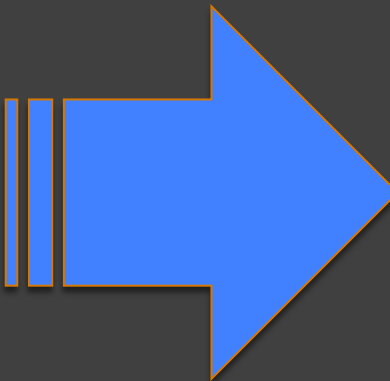
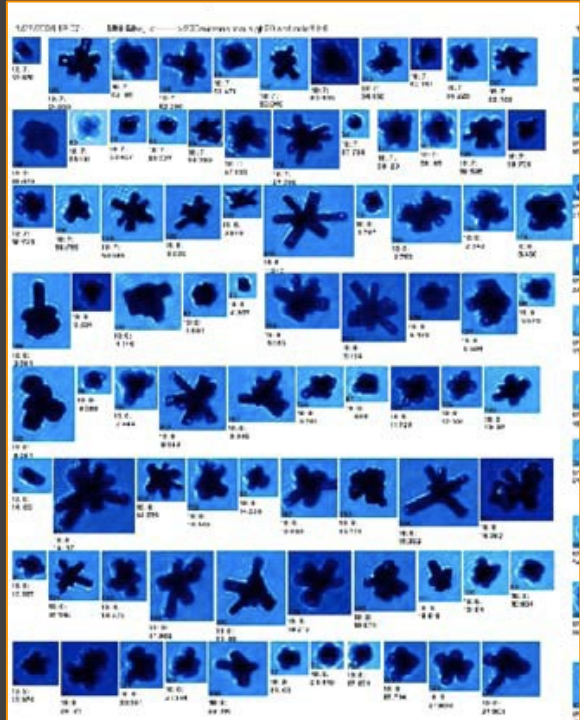
cf. Fu et al. 1996; Fu 2007

Complex vs simple ice crystals

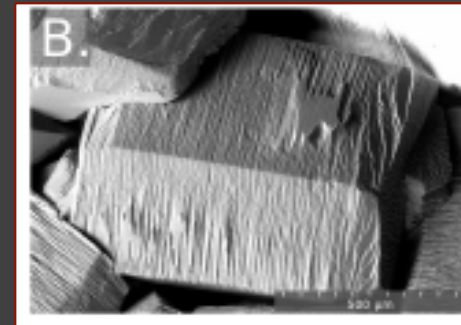
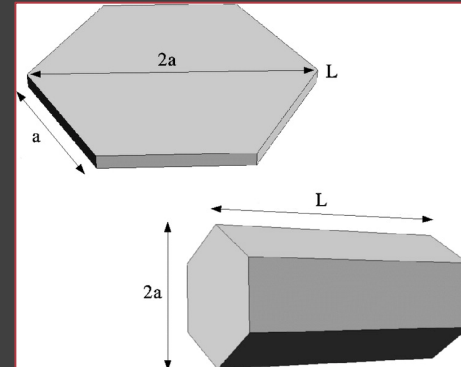


Phase function of complex crystal is similar to phase function of its components (Fu 2007; Um & McFarquhar 2007; 2009)

In summary: Simple radiative proxies for complex ice



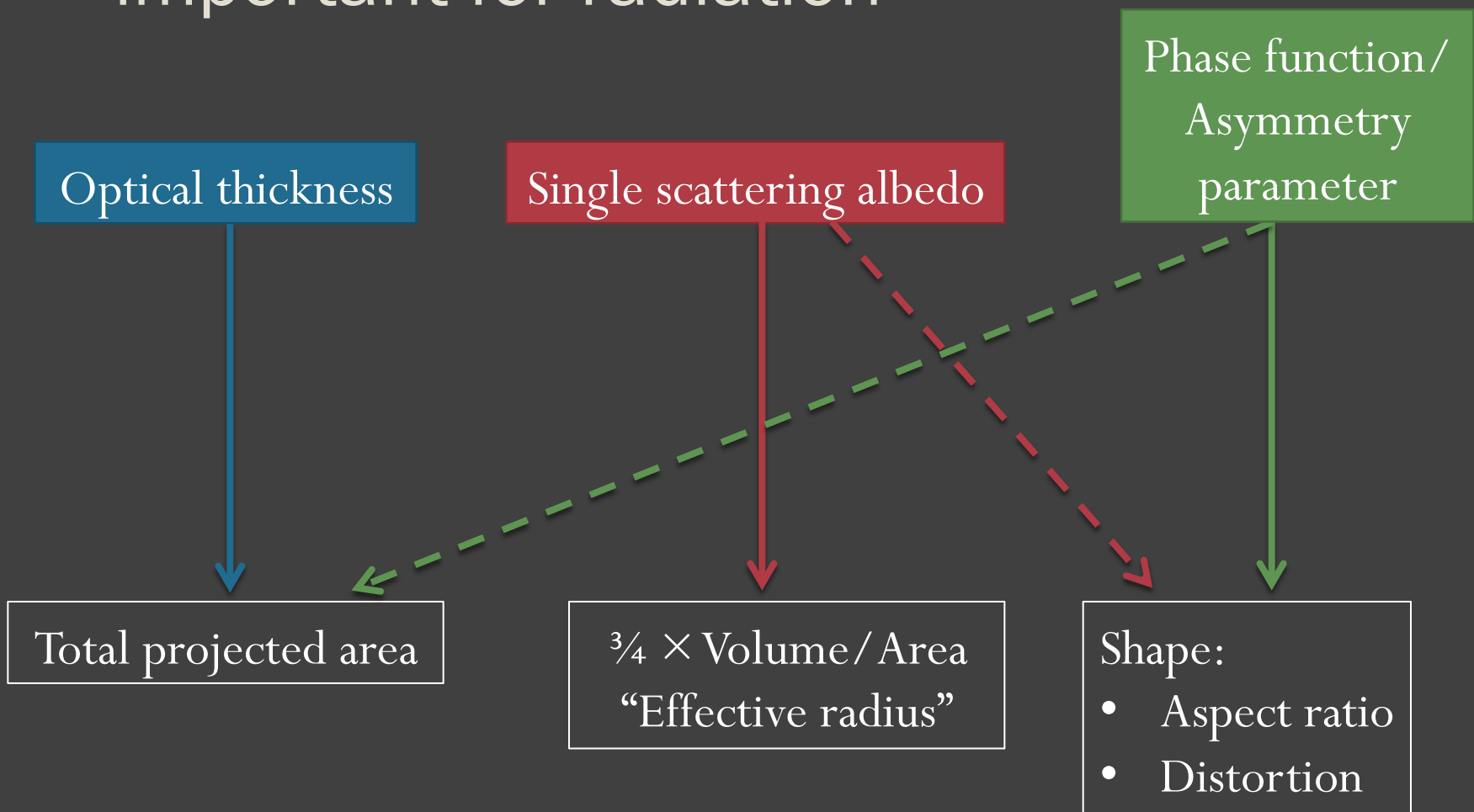
Complex aggregates of plate-like or column-like crystals with varying aspect ratio and distortion



Single hexagonal columns and plates with matching aspect ratio and distortion

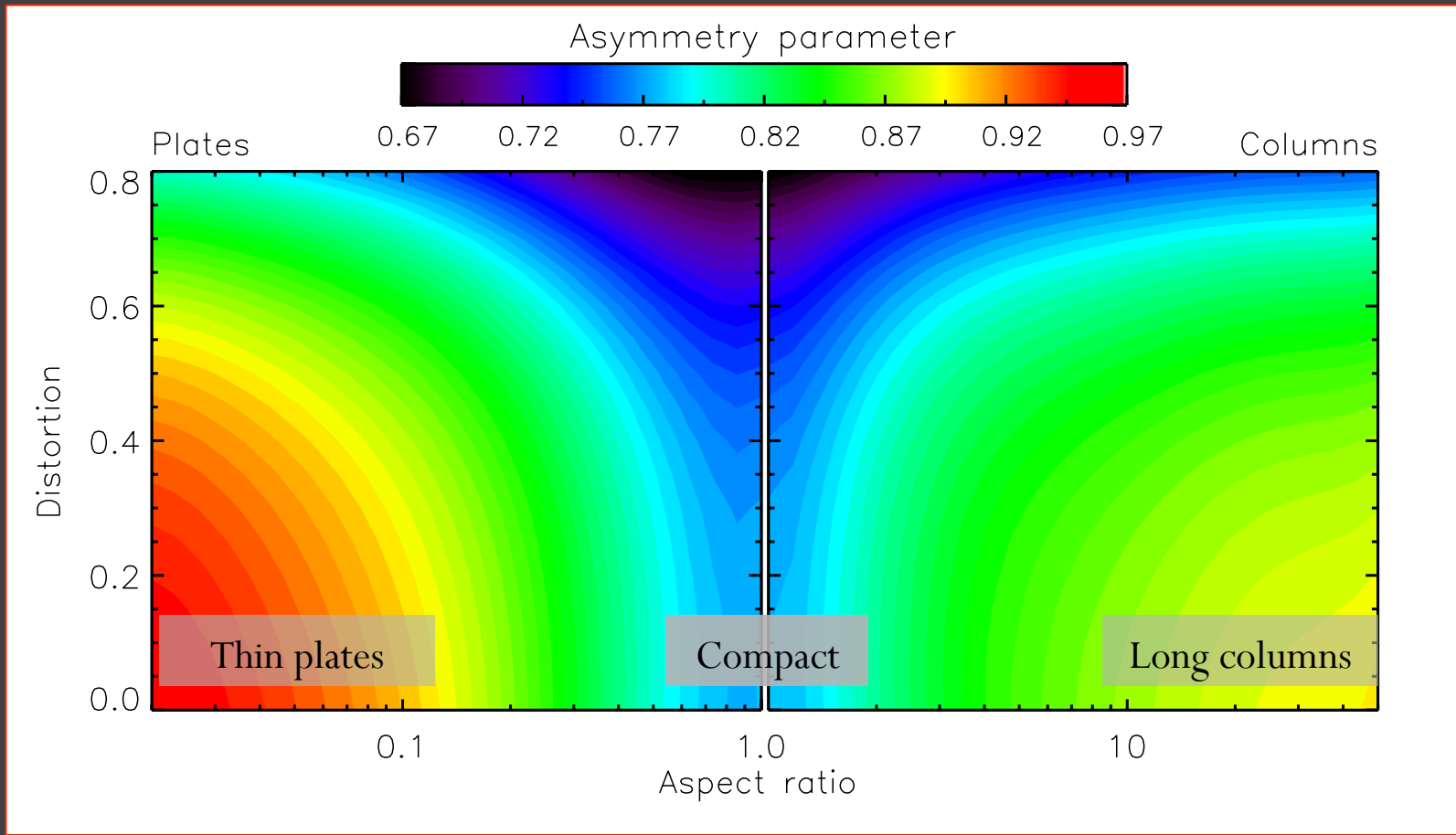
- Optical phenomena
 - van Diedenhoven: *The prevalence of the 22° halo in cirrus clouds*, JQSRT, in press
- Optical properties
 - Van Diedenhoven, B., A.S. Ackerman, B. Cairns, and A.M. Fridlind: *A flexible parameterization for shortwave optical properties of ice crystals*, J. Atmos. Sci., in press
- Remote sensing
 - Van Diedenhoven, B., B. Cairns, I.V. Geogdzhayev, A.M. Fridlind, A.S. Ackerman, P. Yang, and B.A. Baum: *Remote sensing of ice crystal asymmetry parameter using multi-directional polarization measurements — Part 1: Methodology and evaluation with simulated measurements*, Atmos. Meas. Tech., 2012
 - Van Diedenhoven, B., B. Cairns, A.M. Fridlind, A.S. Ackerman, and T.J. Garrett: *Remote sensing of ice crystal asymmetry parameter using multi-directional polarization measurements — Part 2: Application to the Research Scanning Polarimeter*. Atmos. Chem. Phys., 2013

Ice crystal microphysical properties important for radiation

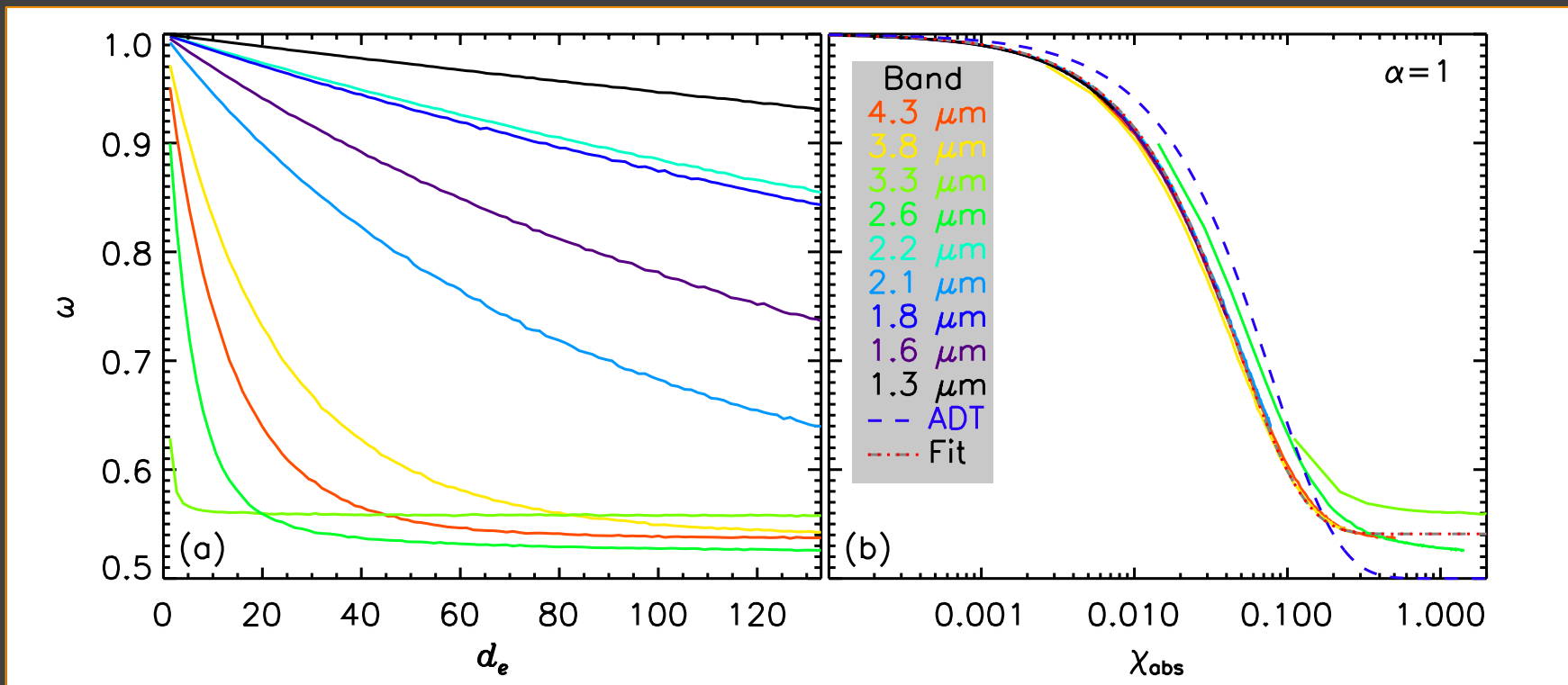


cf. Fu et al. 1996; Fu 2007

2-step 2-D fitting of ice crystal asymmetry parameter



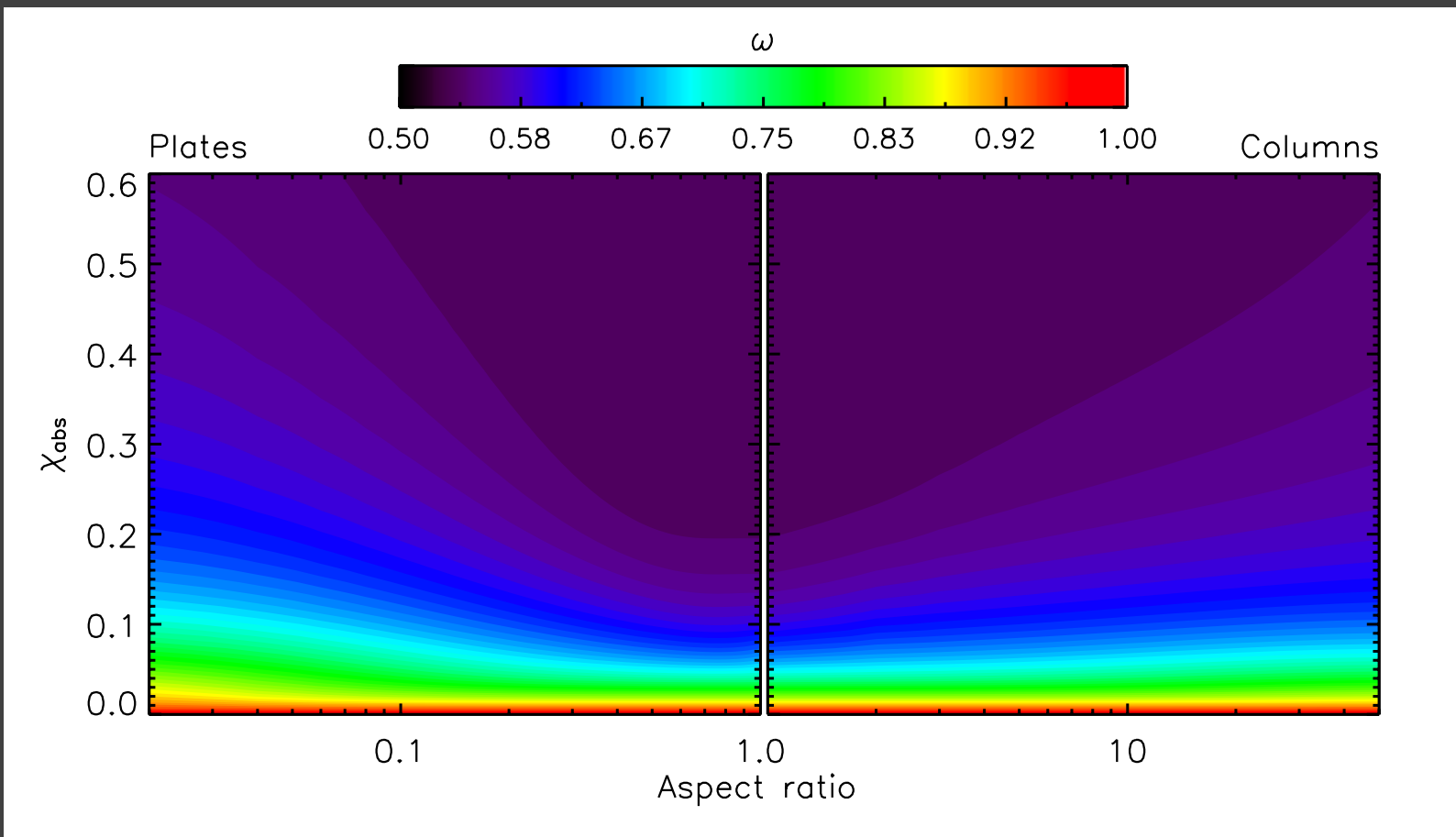
Single scattering albedo

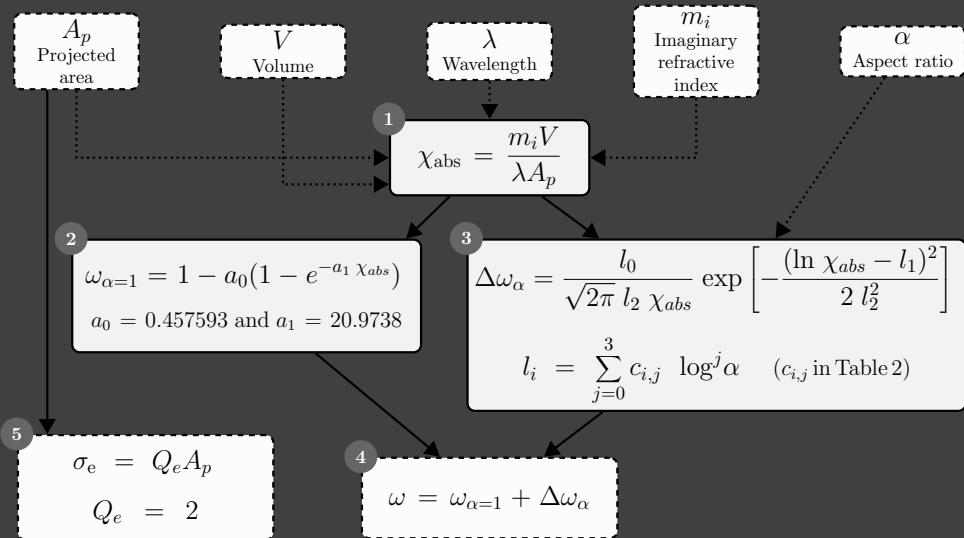


$$d_e = \frac{V}{A_p}.$$

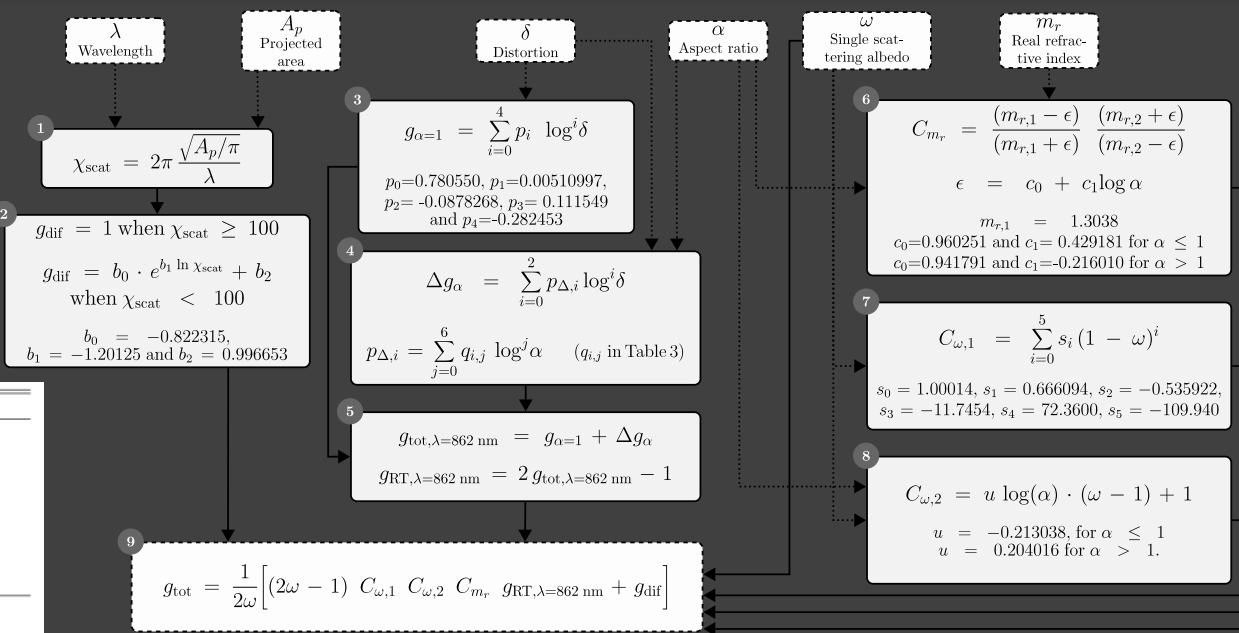
$$\chi_{abs} = \frac{m_i V}{\lambda A_p} = \frac{m_i}{\lambda} d_e,$$

2-step 2-D fitting of single scattering albedo





	j	$c_{0,j}$	$c_{1,j}$	$c_{2,j}$
Plates	0	0.000527060	0.309748	-2.58028
	1	0.00867596	-0.650188	-1.34949
	2	0.0382627	-0.198214	-0.674495
	3	0.0108558	-0.0356019	-0.141318
Columns	0	0.000378774	0.390452	-2.36821
	1	0.00463283	0.420040	1.07603
	2	0.00593106	-0.0848059	-0.729980
	3	-0.00117167	0.0186601	0.232446



	j	$q_{0,j}$	$q_{1,j}$	$q_{2,j}$
Plates	0	-0.00133106	-0.000782076	0.00205422
	1	0.0408343	-0.00162734	0.0240927
	2	0.525289	0.418336	-0.818352
	3	0.443151	1.53726	-2.40399
	4	0.00852515	1.88625	-2.64651
	5	-0.123100	0.983854	-1.29188
Columns	6	-0.0376917	0.187708	-0.235359
	0	-0.00189096	0.000637430	0.00157383
	1	0.00981029	0.0409220	0.00908004
	2	0.732647	0.0539796	-0.665773
	3	-1.59927	-0.500870	1.86375
	4	1.54047	0.692547	-2.05390
	5	-0.707187	-0.374173	1.01287
	6	0.125276	0.0721572	-0.186466

Simple code

- Single scattering albedo, asymmetry parameter for any
 - Volume
 - Projected area
 - Aspect ratio
 - Distortion parameter
 - Wavelength
- Being implemented in the GISS cloud resolving model (CRM)
- In GISS GCM!?

The screenshot shows a code editor window with the following details:

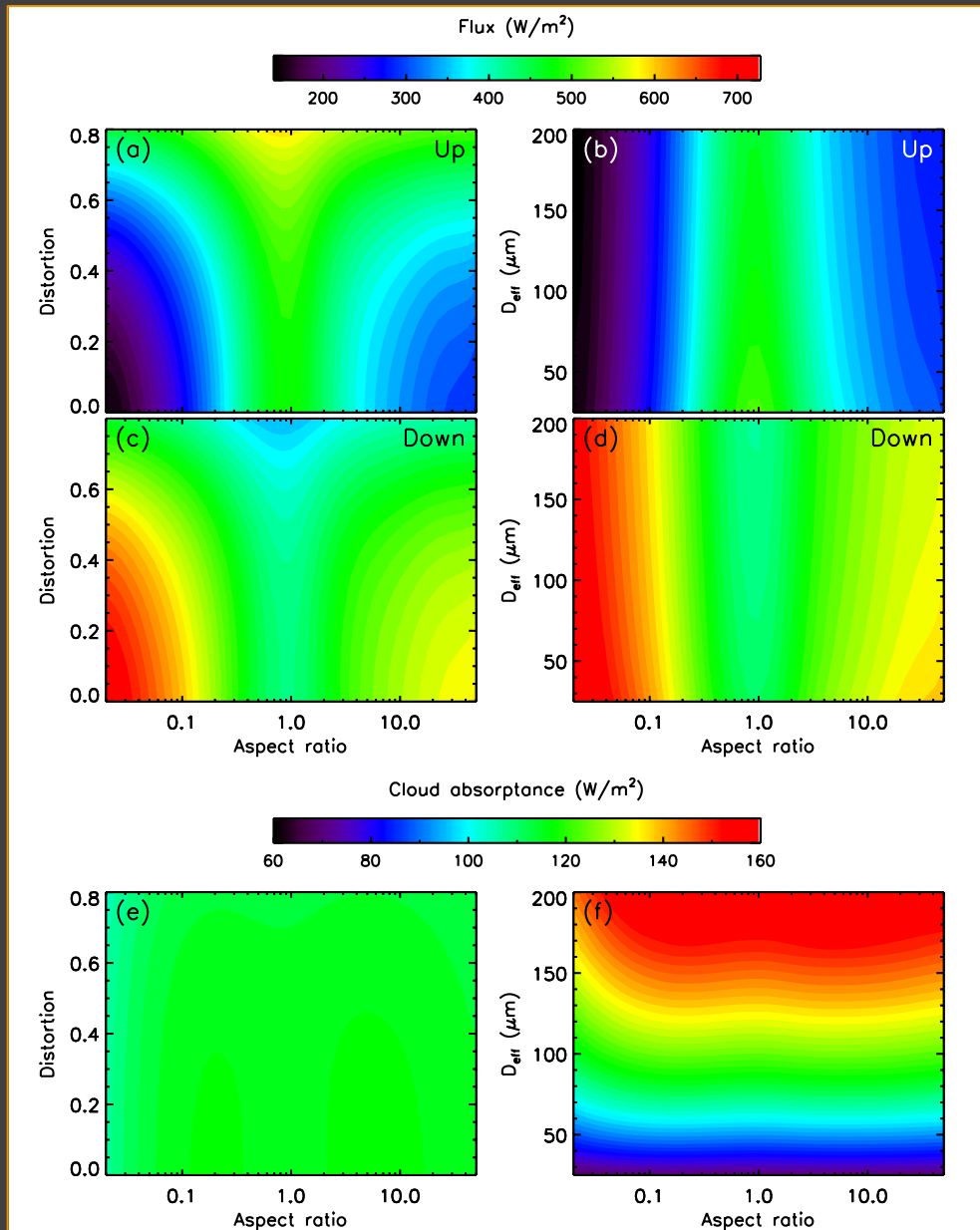
- Title Bar:** ice_OP_parameterization_nocomments.py
- Code Content:** A Python script containing calculations for single scattering albedo and asymmetry parameter. It uses various mathematical operations like logarithms, exponentials, and matrix multiplication. The script includes comments and sections for "SINGLE SCATTERING ALBEDO" and "ASYMMETRY PARAMETER".
- Status Bar:** U:**- ice_OP_parameterization_nocomments.py All L41 (Python)
Beginning of buffer

```
#-----  
#----- SINGLE SCATTERING ALBEDO -----  
#-----  
  
if Chi_abs > 0:  
    w_1= 1.- a[0] * (1.-np.exp(-Chi_abs*a[1]))  
    l=np.zeros(nc1)  
    for i in range(ncl2): l[:] += c_ij[:,i,col_pla] * np.log10(ar)**i  
    D_w= l[0]*np.exp( -(np.log( Chi_abs ) - l[Z] )**2 / (2.*l[1]**2))/( Chi_abs *l[1]*np.sqrt(2.*np.pi))  
    w = w_1 + D_w  
else:  
    w = 1.  
  
#-----  
#----- ASYMMETRY PARAMETER -----  
#-----  
g_diffr = b_gdiff[0] * np.exp(b_gdiff[1]*np.log(Chi_scat)) + b_gdiff[2]  
g_diffr = max([g_diffr,0.5])  
  
g_1 = 0.  
for i in range(len(p_a_eq_1)): g_1 += p_a_eq_1[i]*delta**i  
  
p_delta=np.zeros(nq1)  
for i in range(nq2): p_delta += q_ij[:,i,col_pla]*np.log10(ar)**i  
Dg = 0.  
for i in range(nq1): Dg += p_delta[i]*delta**i  
g_rt = 2.*(g_1 + Dg)-1.  
  
epsilon = c_g[0,col_pla]+c_g[1,col_pla]*np.log10(ar)  
mr1 = 1.3038  
C_m = (mr1-epsilon)/(mr1+epsilon)*(mr+epsilon)/(mr-epsilon)  
  
if Chi_abs > 0:  
    C_w0 = 0.  
    for i in range(len(s)): C_w0 += s[i]*(1.-w)**i  
    k = np.log10(ar)*u[col_pla]  
    C_w1 = k*w-k+1.  
    C_w = C_w0*C_w1  
else: C_w = 1.  
  
g_rt_corr = g_rt*C_m*C_w  
  
g_tot = 1./(2.*w)*( (2.*w-1.)*g_rt_corr + g_diffr )  
g_tot = min([g_tot,1.])
```

Solar Flux variations from varying size and shape

- Optical thickness = 4
- SZA= 60°

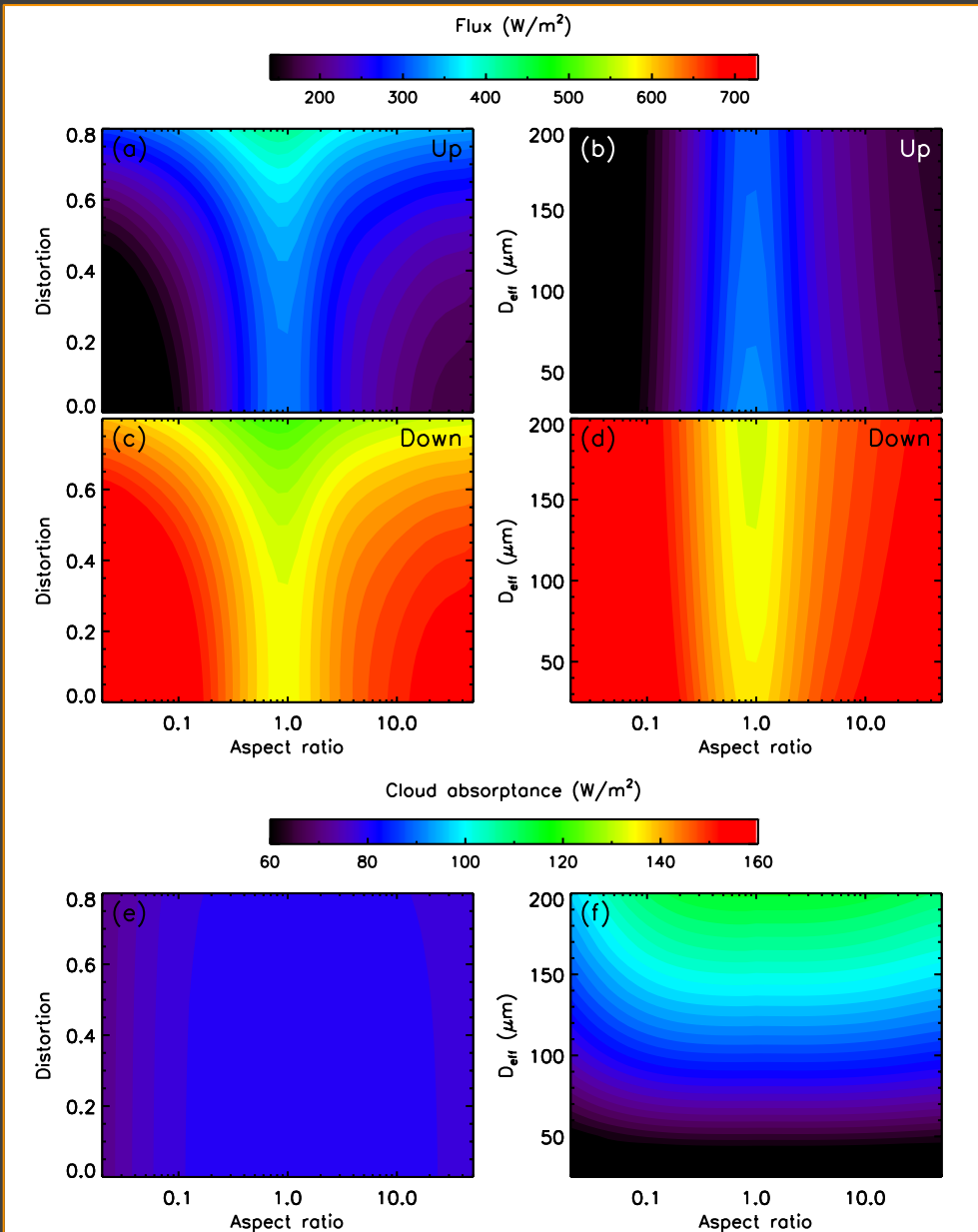
van Diedenhoven et al., “A flexible parameterization for shortwave optical properties of ice crystals”, JAS, in press



Solar Flux variations from varying size and shape

- Optical thickness = 2
- SZA= 60°

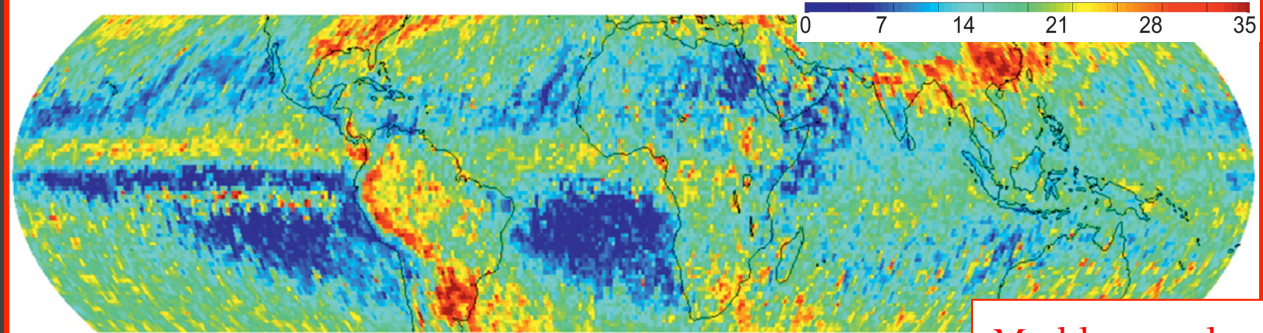
van Diedenhoven et al., “A flexible parameterization for shortwave optical properties of ice crystals”, JAS, in press



- Optical phenomena
 - van Diedenhoven: *The prevalence of the 22° halo in cirrus clouds*, JQSRT, in press
- Optical properties
 - Van Diedenhoven, B., A.S. Ackerman, B. Cairns, and A.M. Fridlind: *A flexible parameterization for shortwave optical properties of ice crystals*, J. Atmos. Sci., in press
- Remote sensing
 - Van Diedenhoven, B., B. Cairns, I.V. Geogdzhayev, A.M. Fridlind, A.S. Ackerman, P. Yang, and B.A. Baum: *Remote sensing of ice crystal asymmetry parameter using multi-directional polarization measurements — Part 1: Methodology and evaluation with simulated measurements*, Atmos. Meas. Tech., 2012
 - Van Diedenhoven, B., B. Cairns, A.M. Fridlind, A.S. Ackerman, and T.J. Garrett: *Remote sensing of ice crystal asymmetry parameter using multi-directional polarization measurements — Part 2: Application to the Research Scanning Polarimeter*. Atmos. Chem. Phys., 2013

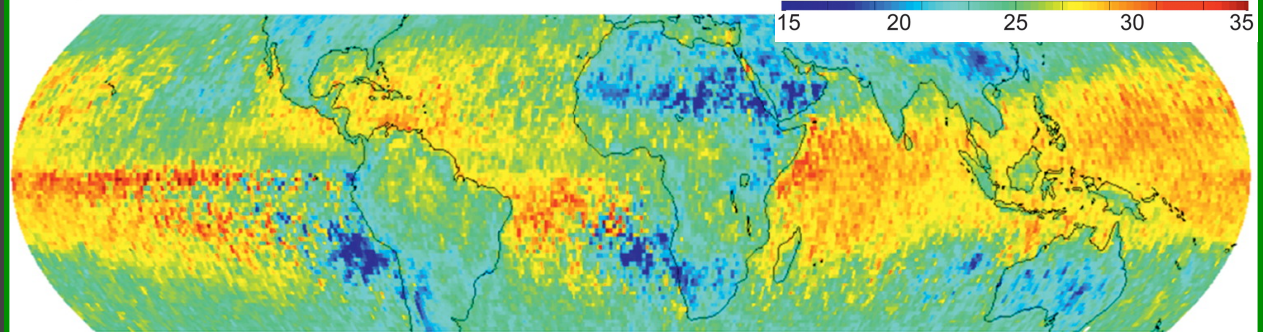
Current
knowledge on
fundamental
global ice
cloud optical
properties

e) Cloud Optical Thickness Ice



Maddux et al.,
JAOT 2010

c) Cloud Effective Radius Ice (μm)



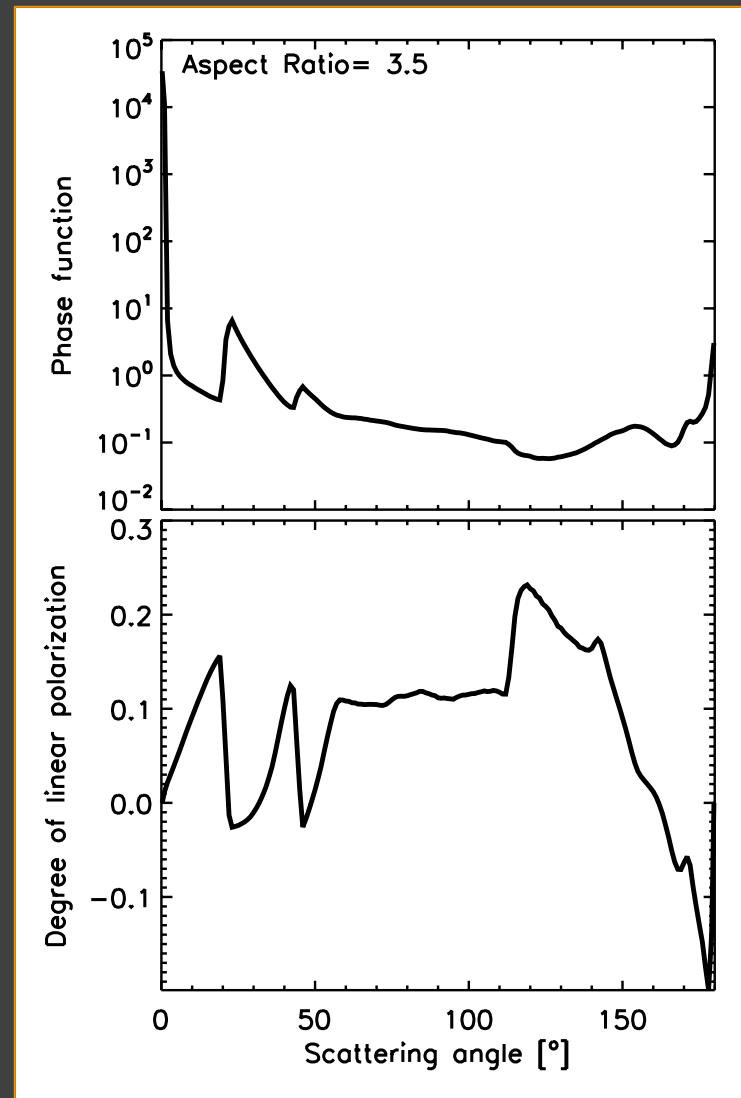
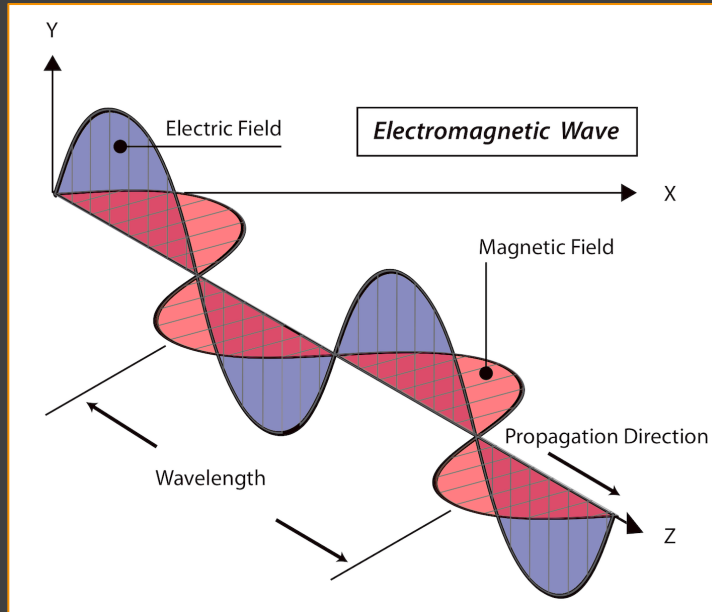
???

Asymmetry Parameter

???

A little help from polarization

- Orientation of EM wave
- A single scattering event on ice crystals polarizes light
- Multiple scattering wipes out any polarization



Information from Polarization

Polarization contains info about

- Aspect ratio (AR)
- Distortion δ (Macke et al. 1996)

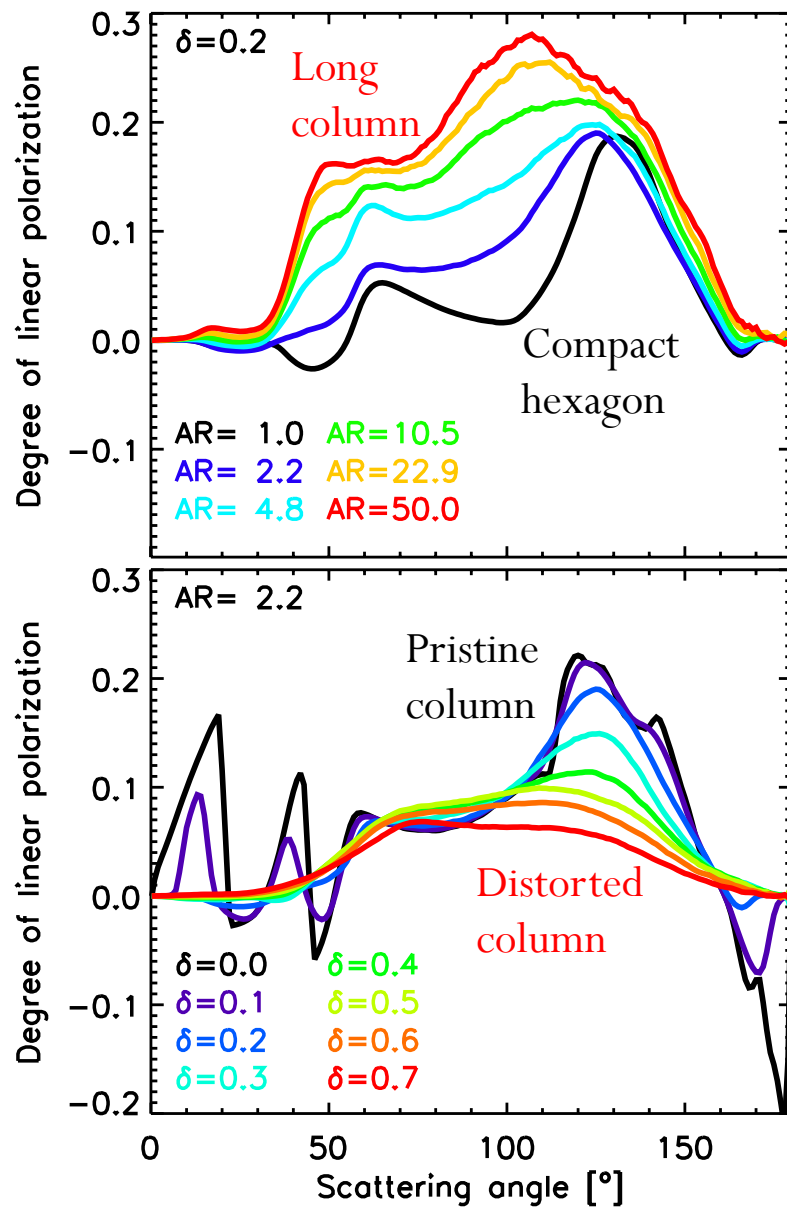
Multi-directional polarized
reflectance measurements

conserve

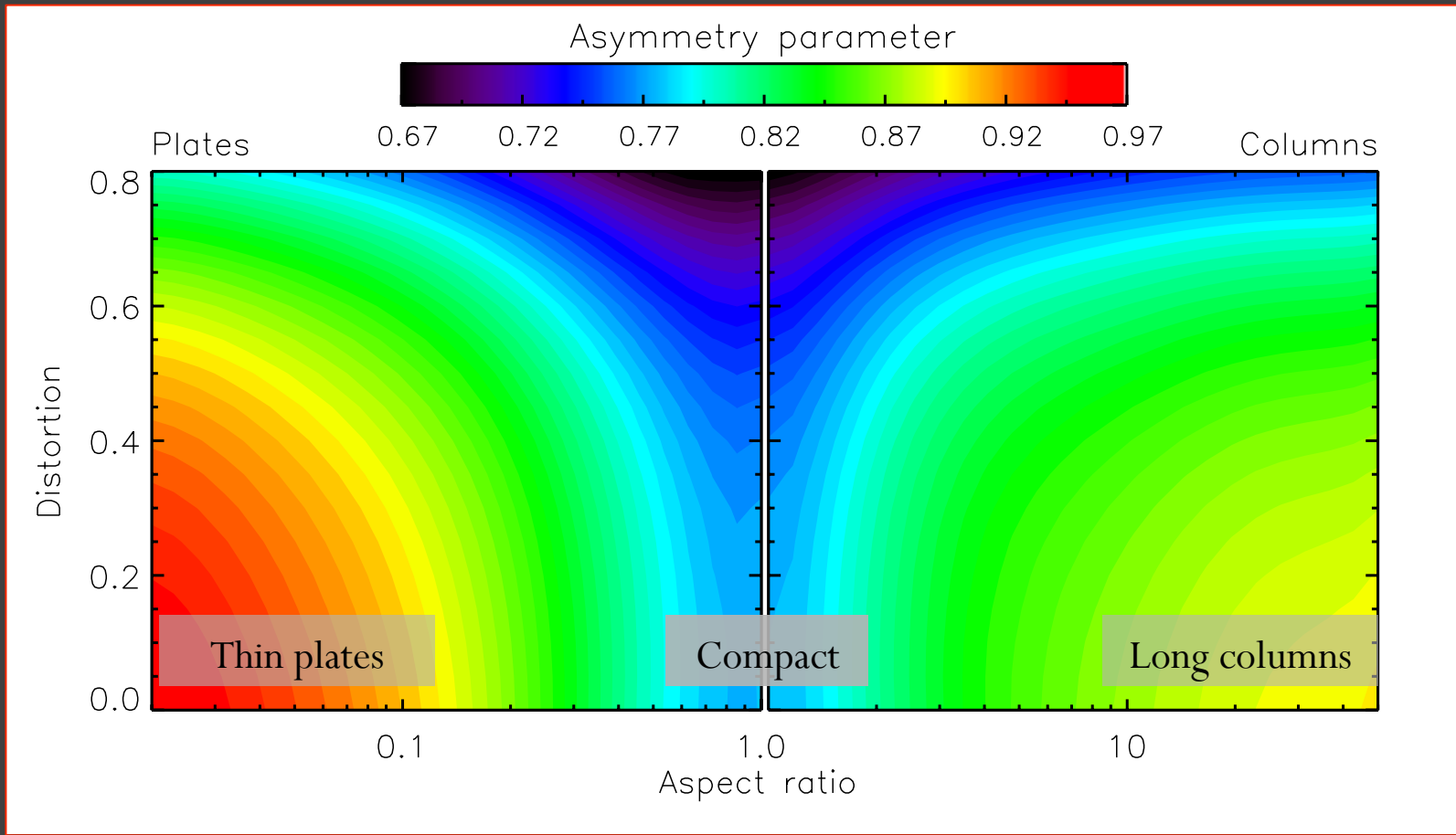
Single scattering features

Retrieve aspect ratio and
distortion from polarization to
estimate asymmetry parameter

van Diedenhoven et al., Atmos. Meas. Tech., 2012



Ice crystal asymmetry parameter dependence on aspect ratio and distortion

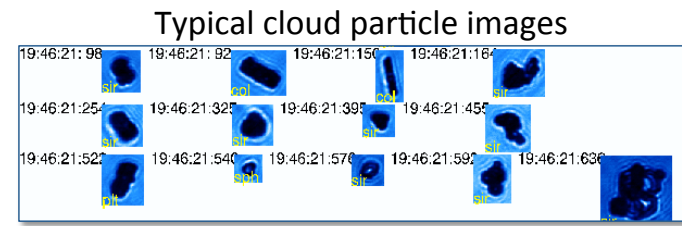
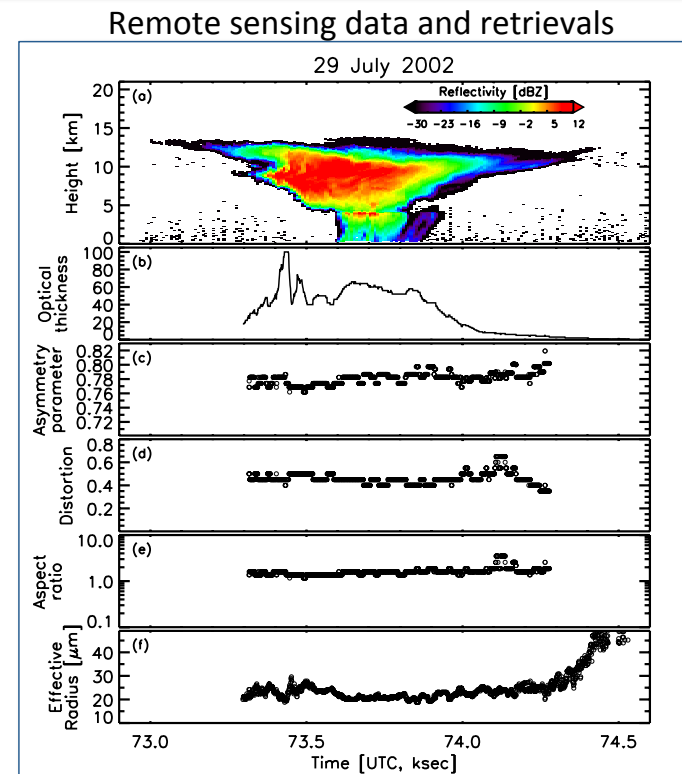
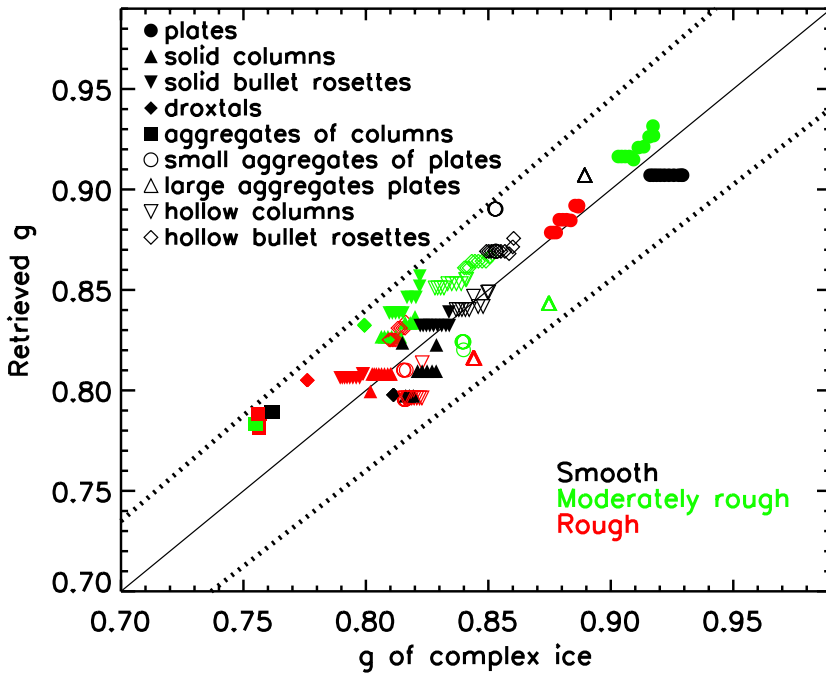


Tests

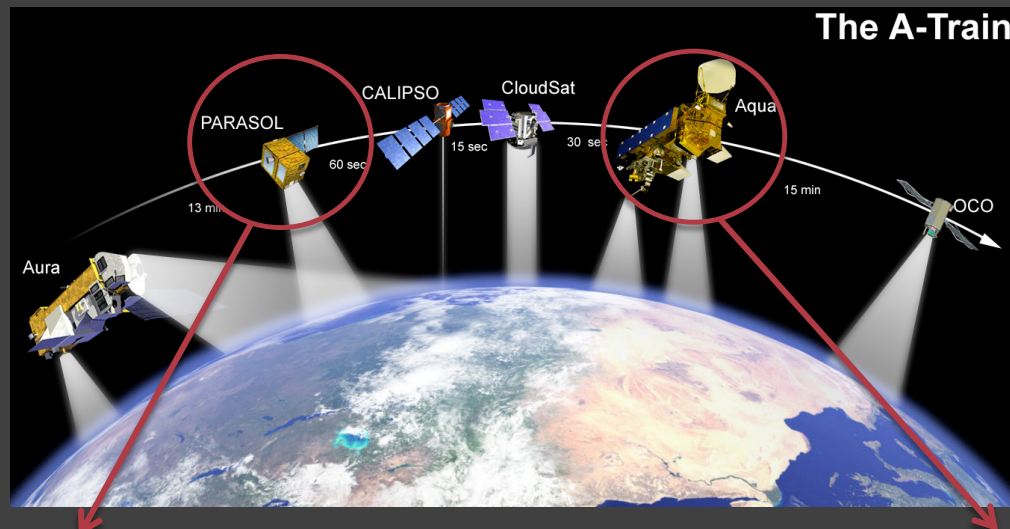
Research scanning Polarimeter :
RSP data collected during CRYSTAL-FACE

Simulated data:

- Complex ice shapes (Yang et al.)
- 20 different size distributions
- Retrieval within 5% (0.04),
Mean bias: 0.004



Towards global retrievals: POLDER/PARASOL and MODIS/Aqua



POLDER

- Multi-angle polarization measurements
- up to 16 angles per pixel
- No ice-absorbing wavelength bands



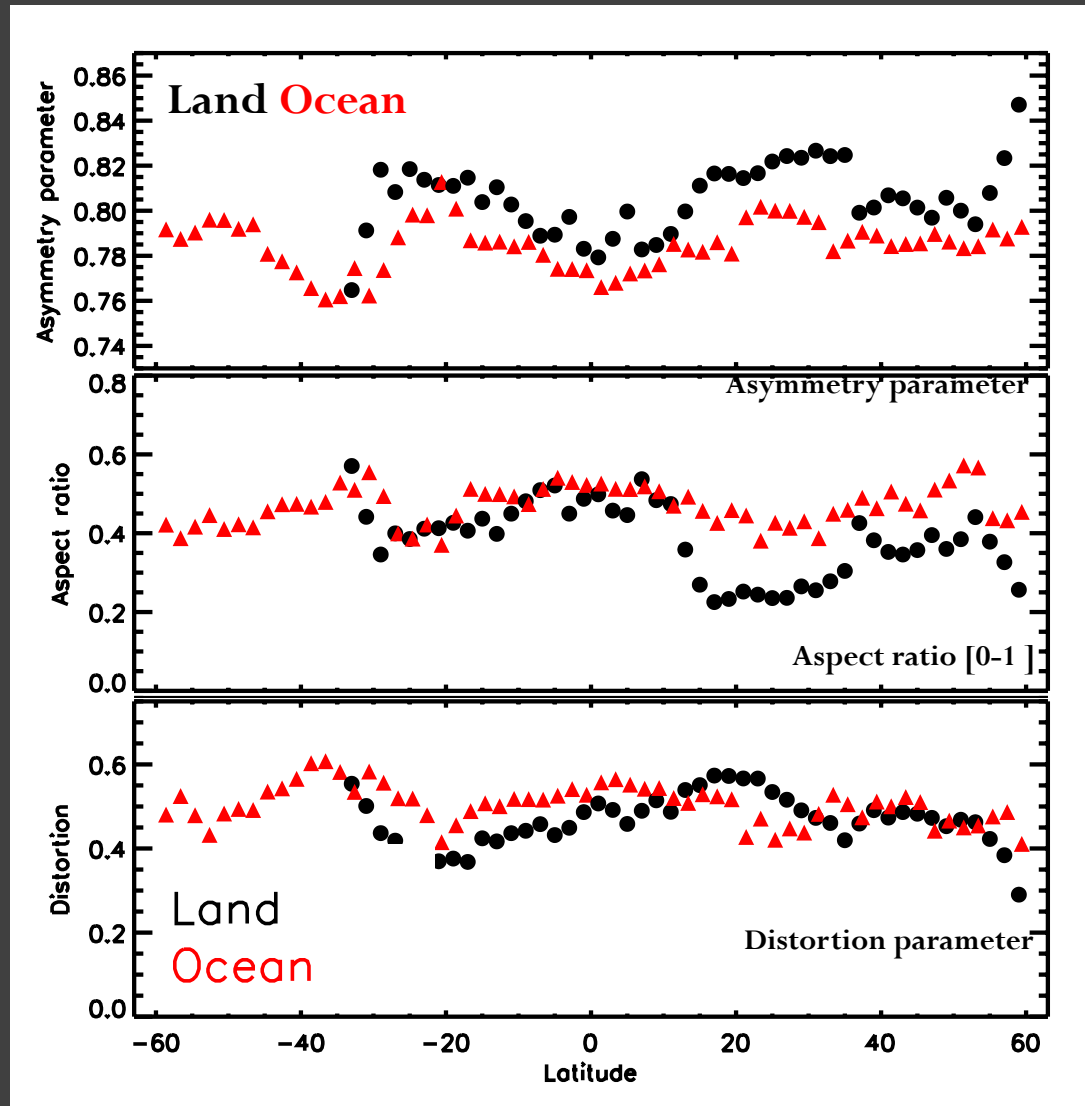
MODIS

- Multi-wavelength imager
- ice-absorbing wavelength bands
- Infrared bands to retrieve cloud height



Preliminary global results

- Only COT>5
- 3 days in January, 3 days in June
 - Tropics: $g \sim 0.76-0.8$
 - mid-latitudes: $g \sim 0.76-0.8$
 - $10-30^\circ$: $g \sim 0.78-0.83$
- $g \sim 0.02$ greater over land
- Low aspect ratios North of 15°
- Mostly plate-like
- Highly distorted $\delta \sim 0.5$



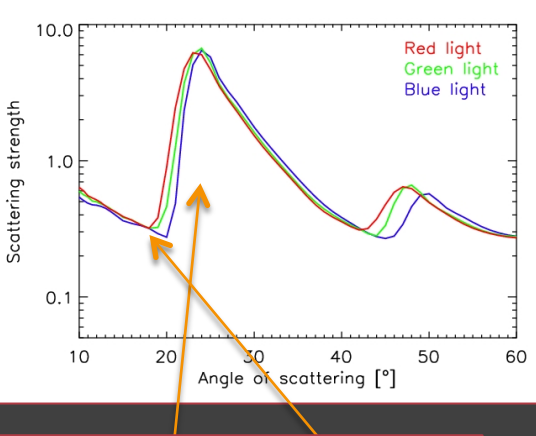
- Optical phenomena
 - van Diedenhoven: *The prevalence of the 22° halo in cirrus clouds*, JQSRT, in press
- Optical properties
 - Van Diedenhoven, B., A.S. Ackerman, B. Cairns, and A.M. Fridlind: *A flexible parameterization for shortwave optical properties of ice crystals*, J. Atmos. Sci., in press
- Remote sensing
 - Van Diedenhoven, B., B. Cairns, I.V. Geogdzhayev, A.M. Fridlind, A.S. Ackerman, P. Yang, and B.A. Baum: *Remote sensing of ice crystal asymmetry parameter using multi-directional polarization measurements — Part 1: Methodology and evaluation with simulated measurements*, Atmos. Meas. Tech., 2012
 - Van Diedenhoven, B., B. Cairns, A.M. Fridlind, A.S. Ackerman, and T.J. Garrett: *Remote sensing of ice crystal asymmetry parameter using multi-directional polarization measurements — Part 2: Application to the Research Scanning Polarimeter*. Atmos. Chem. Phys., 2013



Why are 22 degree halos so common
although ice crystals seem mostly non-
pristine?

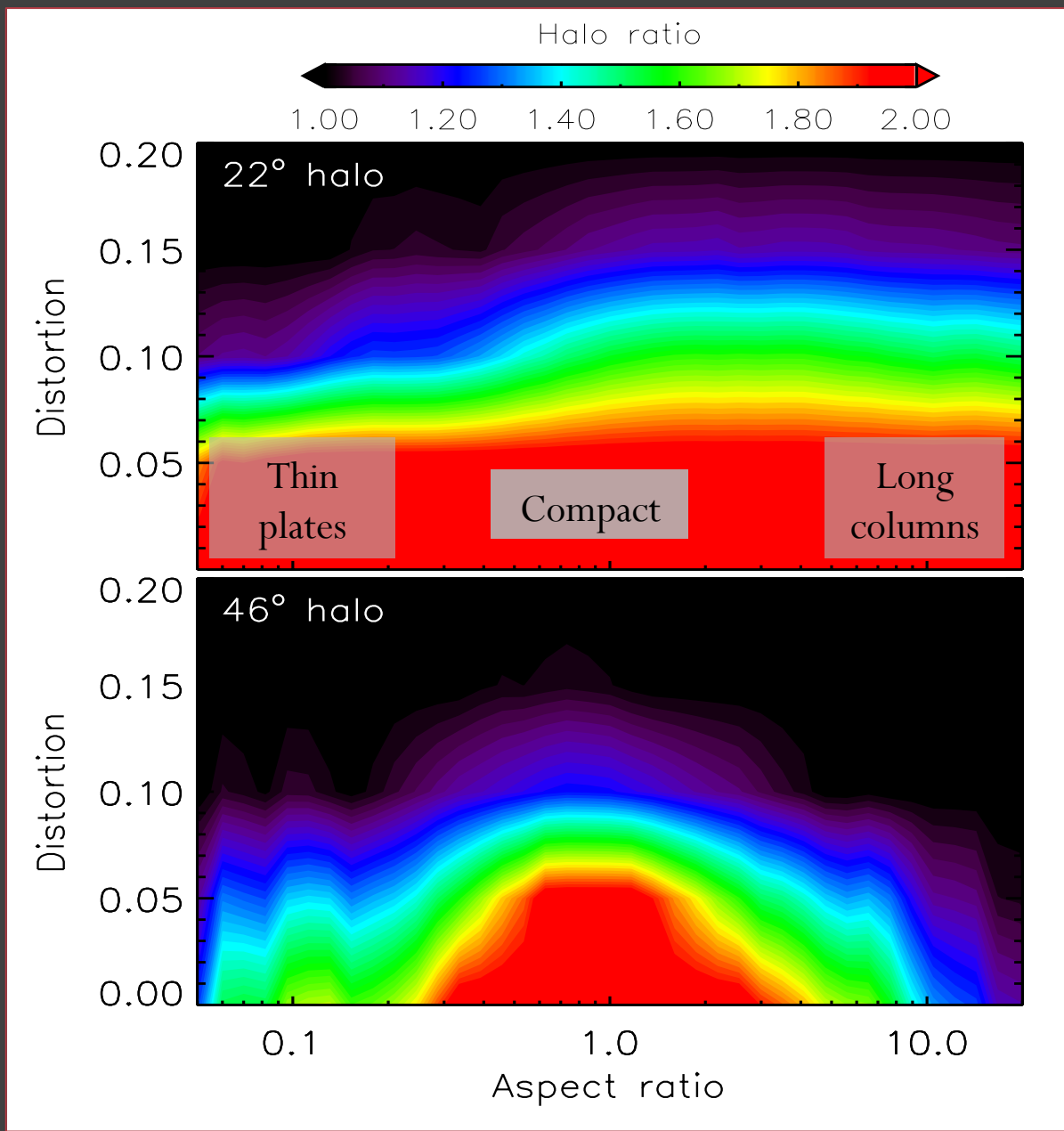
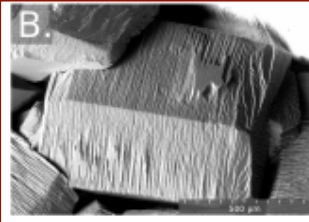
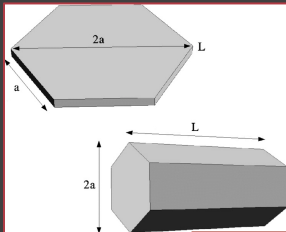


Halo ratios



$$h_{22} = P(22^\circ) / P(18.5^\circ)$$

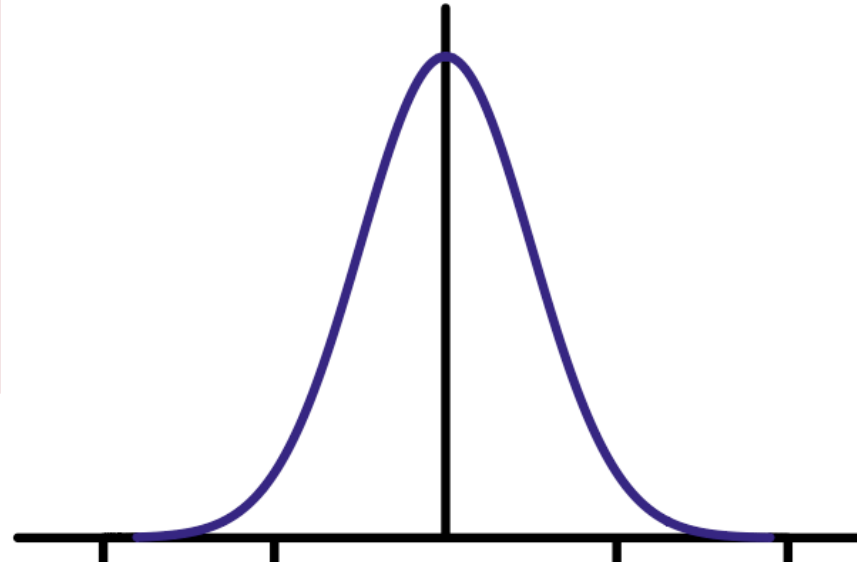
(Shcherbakov, JQSRT, 2013)

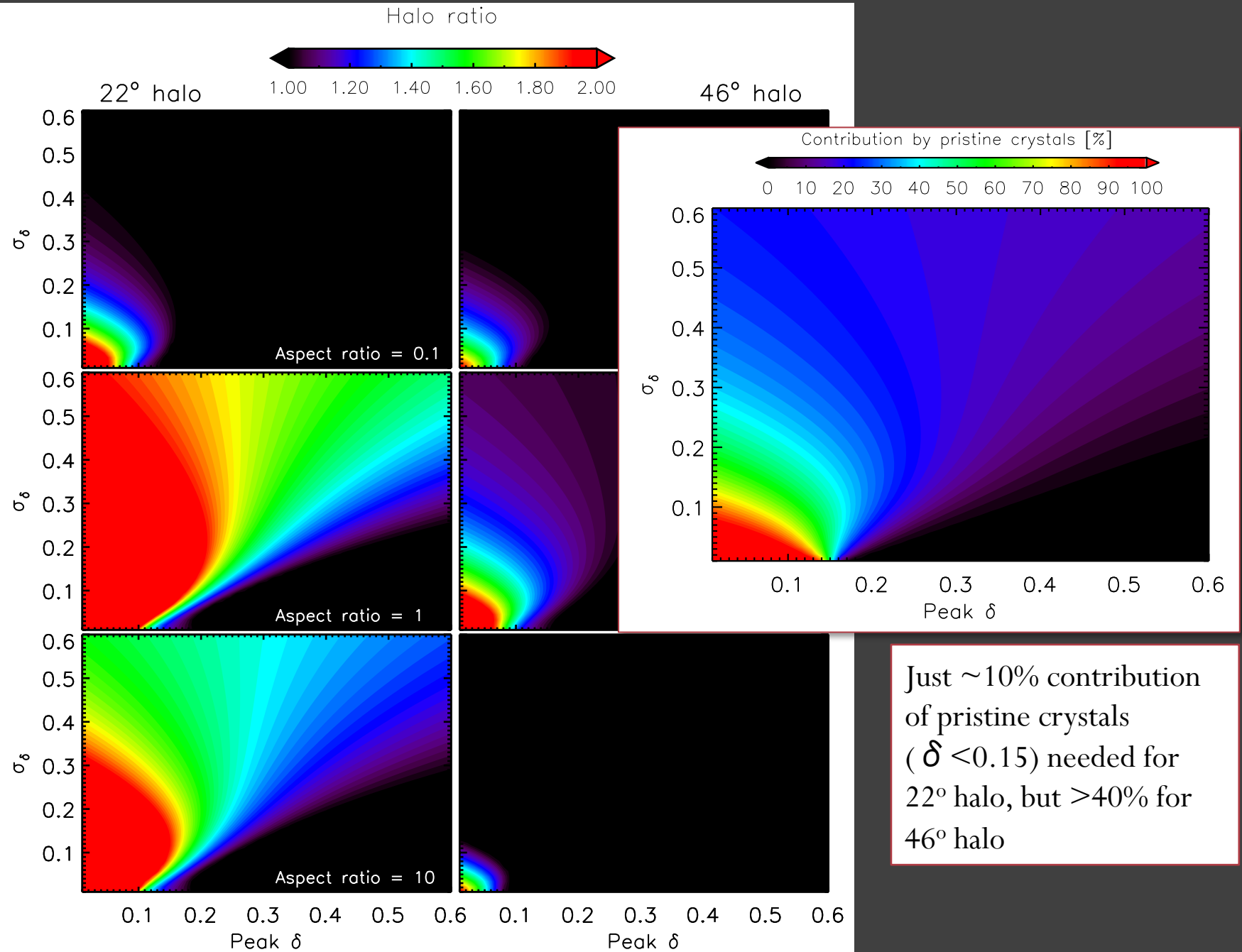


12/20/2010 005715--180340 <----->200microns focus gt 20 and cutoff lt 6



How persistent are the halo features in a mix of distorted and pristine crystals?





Summary

- Simple hexagonal plates and columns serve as radiative proxies for complex ice
- Parameterization of optical properties of ice crystals for any combination of
 - Volume
 - Projected area
 - Aspect ratio
 - Distortion
 - Wavelength
- Remote sensing of ice aspect ratio, distortion and asymmetry parameter using multi-directional polarized reflectances
- 22-degree halo is very persistent in a mix of distorted and pristine crystals

Clouds associated with Superstorm Sandy's outflow

Huntsville, AL, Oct. 30, 2012
(Earth Science Picture of the
Day, Nov. 12, 2012)



Bastiaan.vanDiedenhoven@nasa.gov

Resources: www.atoptics.co.uk, Snowcrystals.com

<http://www.atoptics.co.uk/>

Less frequently seen halos

An all sky HaloSim simulation for a 26° high sun and very well aligned cloud crystals.

Some of these halos might be expected to be visible on average more than once a year. Others are once in a lifetime sights.

Click the halo key to reach descriptions.

The diagram illustrates a halo simulation for a 26° high sun using well-aligned cloud crystals. It shows concentric arcs and other optical phenomena. Labels point to specific features:

- Diffuse arcs
- Anthelion
- Tricker arc
- 120° parhelion
- Subhelic arc
- Hastings arc
- Wegener arc
- Supralateral arc
- 46° halo
- Infralateral arc
- Parry supralateral
- Parry arc
- Parry infralateral
- Heliac arc



<http://www.atoptics.co.uk/>



Bastiaan.vanDiedenhoven@nasa.gov

Resources: www.atoptics.co.uk, Snowcrystals.com



Bastiaan.vanDiedenhoven@nasa.gov

Bi, L., P.Yang, C Liu, BYi, B.A. Baum, B. van Diedenhoven, and H. Iwabuchi, 2014:

Assessment of the accuracy of the conventional ray-tracing technique: Implications in remote sensing and radiative transfer involving ice clouds. *J. Quant. Spectrosc. Radiat. Transfer*, submitted.

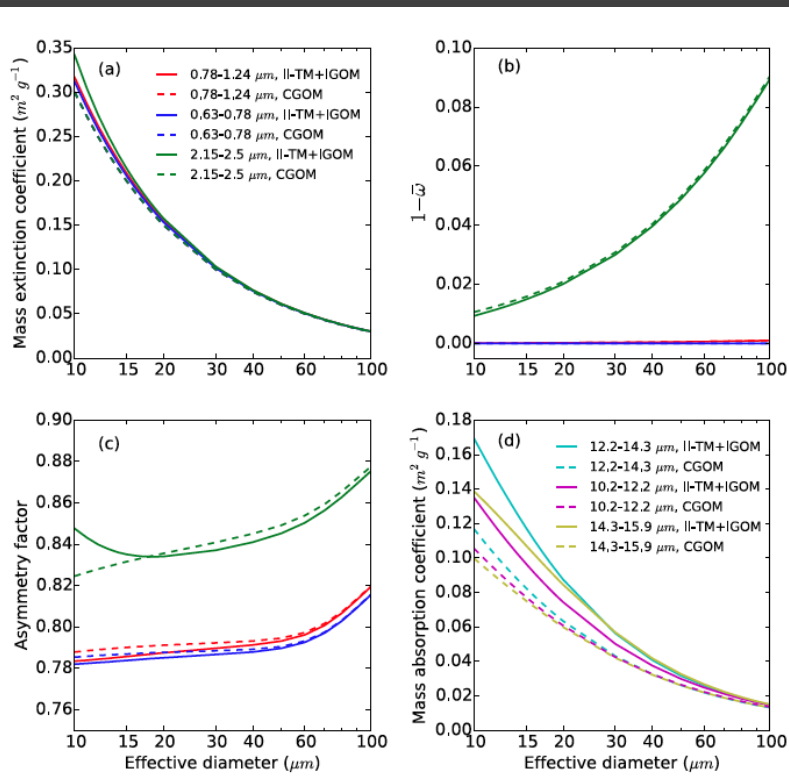


Fig.11. Comparison of bulk ice cloud optical properties derived from II-TM+IGOM and CGOM at selected spectral bands of the RRTMG RTM.

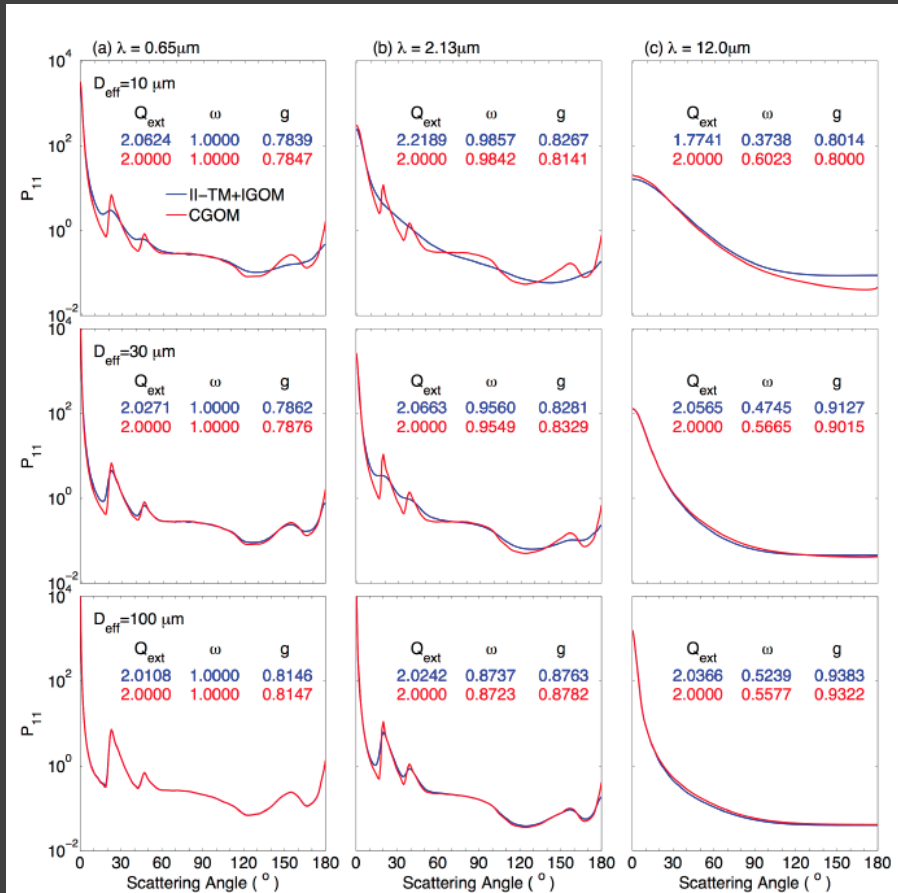


Fig. 5. Comparison of bulk ice cloud scattering phase functions for different effective diameters at the wavelengths of (a) $0.65 \mu m$ (left column), (b) $2.13 \mu m$ (middle column), and (c) $12.0 \mu m$ (right column). Indicated in the figure are the bulk extinction efficiency, the bulk single-scattering albedo, and the asymmetry factor of the bulk-scattering phase function.

Bi, L., P.Yang, C Liu, BYi, B.A. Baum, B. van Diedenhoven, and H. Iwabuchi, 2014:

Assessment of the accuracy of the conventional ray-tracing technique: Implications in remote sensing and radiative transfer involving ice clouds. *J. Quant. Spectrosc. Radiat. Transfer*, submitted.

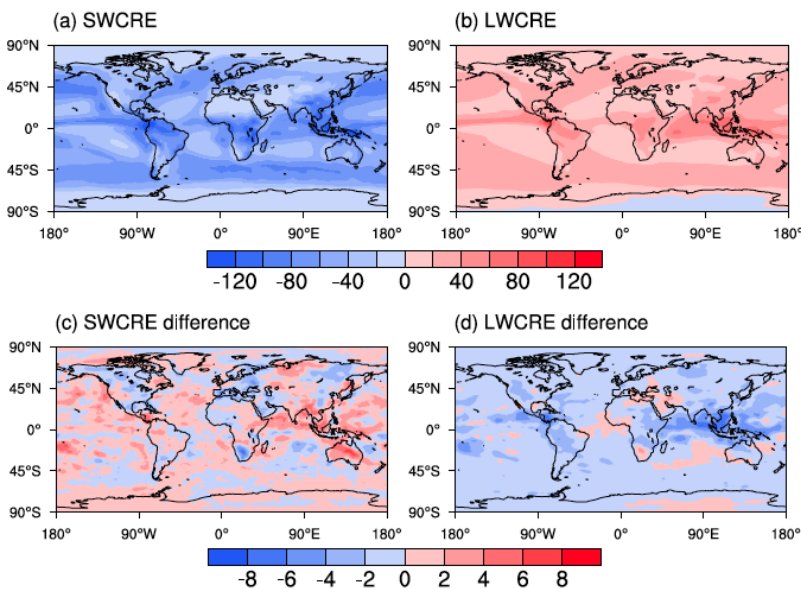


Fig. 14. Ten-year mean annual SW/LW total cloud radiative effect (unit: W m^{-2}) and the differences between the II-TM+IGOM and the CGOM cases (the CGOM case minus the II-TM+IGOM case).

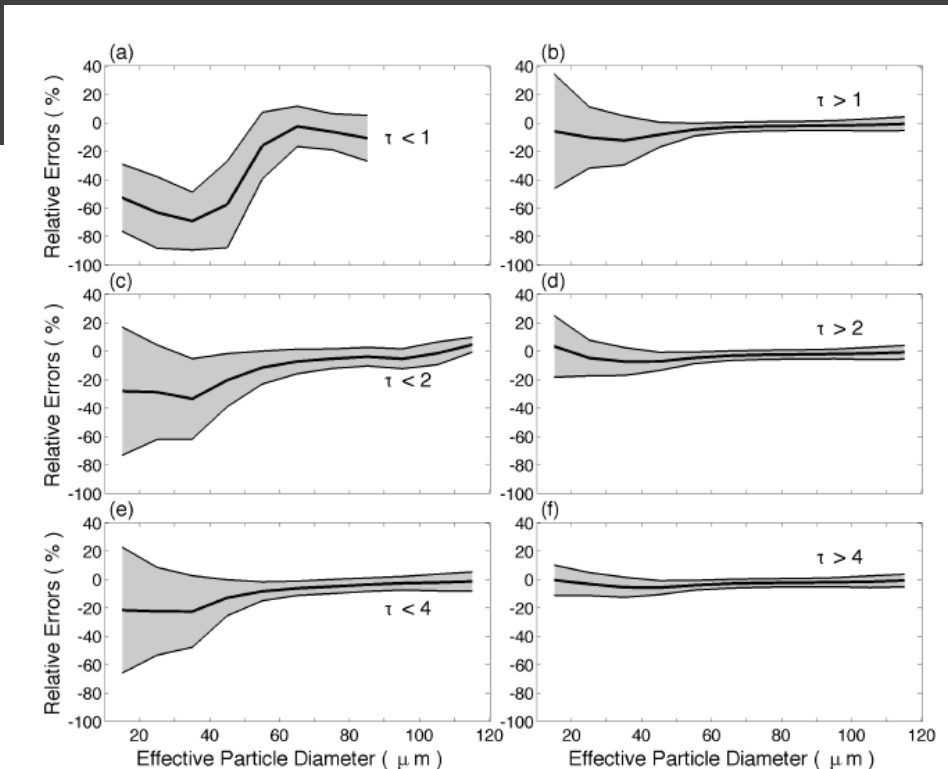


Fig. 9. The mean and standard deviations for the relative errors in the retrieved effective diameter within different ranges of the optical thickness.